Renormalization of the $\Delta B = 2$ four-quark operators in lattice nonrelativistic QCD

S. Hashimoto,[1] K-I. Ishikawa,[1] T. Onogi,[2] M. Sakamoto,[2] N. Tsutsui,[1] and N. Yamada[1]

[1]*High Energy Accelerator Research Organization (KEK), Tsukuba 305-0801, Japan*
[2]*Department of Physics, Hiroshima University, Higashi-Hiroshima 739-8526, Japan*

We calculate perturbative renormalization constants for the $\Delta B = 2$ four-quark operators in lattice NRQCD. Continuum operators $\bar{b}\gamma_\mu(1-\gamma_5)q\bar{b}\gamma_\mu(1-\gamma_5)q$ and $\bar{b}(1-\gamma_5)q\bar{b}(1-\gamma_5)q$, which are necessary in evaluating the mass and width differences in $B^0_{d(s)} - \bar{B}^0_{d(s)}$ systems, are matched at one loop with corresponding lattice operators constructed from the NRQCD heavy quarks and the $\mathcal{O}(a)$-improved light quarks. Using these perturbative coefficients, we also reanalyze our previous simulation results for the matrix elements of the above operators. Our new results are free from the systematic error of $\mathcal{O}(\alpha_s/(aM_b))$ in contrast with the previous ones with matching coefficients evaluated in the static limit.

I. INTRODUCTION

The B meson decay constant and the B parameter in B-$\bar{B}$ mixing are crucial quantities for determining the Cabibbo–Kobayashi–Maskawa (CKM) mixing matrix elements $|V_{td}|$ and $|V_{ts}|$ from the experimental values of the oscillation frequency $\Delta M_{d(s)}$. While the lattice calculation of the decay constant has reached a satisfactory level where the systematic error except for the quenching effect is about 10%, the B parameter B_B still has a large uncertainty of about 30% even in the quenched approximation [1]. Further effort in lattice calculations is required to constrain the CKM matrix elements more tightly.

In the limit of infinitely heavy quark mass, a lattice calculation of the B parameter has been performed by several authors using the static action and the $\mathcal{O}(a)$-improved (or unimproved) light quark actions [2–5], for which the perturbative matching factor of relevant four-quark operators in continuum and lattice definitions is available [6–9]. The problem of a large one-loop coefficient raised in Refs. [2,3] is not essential when used with the tadpole improved perturbation theory [12] as discussed in Refs. [4,5], where they find that the results of several groups are in reasonable agreement.

The next step towards the final prediction is to incorporate the correction from a finite b quark mass M_b, which can be systematically included using p/M_b expansion, where p is the typical momentum of the gluons and quarks. A naive order counting suggests that the correction is about $\Lambda_{QCD}/M_b \sim 10\%$, when the size of the QCD scale is assumed to be around 350 MeV. On the lattice, nonrelativistic QCD (NRQCD) [13] provides a necessary formulation to calculate the p/M_b corrections, and an exploratory lattice calculation of the B meson B parameter has already been made [14,15]. One of the main drawbacks in that calculation is, however, that the one-loop coefficients for the infinitely heavy quark mass are used instead of those for lattice NRQCD. This approximation introduces a large systematic uncertainty of order $\alpha_s/(aM_b)$, which is as large as 10%–20% for a typical value of inverse lattice spacing $1/a \sim 2$ GeV and almost equivalent to or even larger than the physical size of the p/M_b correction itself.

Calculation of B_B using the relativistic lattice actions for heavy quark [16–23] is another possibility to study the finite heavy quark mass correction. These calculations, however, may suffer from large $\mathcal{O}(aM)$ [$\mathcal{O}(\alpha_s aM)$ or $\mathcal{O}((aM)^2)$ for the $\mathcal{O}(a)$-improved actions] systematic error and the uncertainty in the extrapolation to the b quark mass from lighter heavy quark masses, for which simulations are performed.

In this paper, we compute the one-loop renormalization constants for $\Delta B = 2$ four-quark operators constructed with the NRQCD heavy quarks and with the $\mathcal{O}(a)$-improved light quarks on the lattice in order to remove the error of the order $\alpha_s/(aM_b)$ in the lattice calculation of B_B. We consider the leading dimension six operators and neglect dimension seven operators which would remove errors of $\mathcal{O}(\alpha_s\Lambda_{QCD}/M_b)$ or $\mathcal{O}(\alpha_s a\Lambda_{QCD})$. The one-loop coefficient for the dimension seven operators which corresponds to $\mathcal{O}(\alpha_s a\Lambda_{QCD})$ corrections has been obtained in Ref. [9] in the infinitely heavy quark mass limit.

Using the renormalization constants obtained in this work, we reanalyze the simulation data of Ref. [14] to obtain an improved result for B_B, which is free from the large systematic uncertainty of $\mathcal{O}(\alpha_s/(aM_b))$. The central value is increased by about 12% with this new analysis, which is within the size of errors expected by a naive order counting argument.

Another important application of our perturbative work is the lattice calculation of B_S, which is a B parameter necessary to evaluate the width difference in the $B_{(s)}$-$\bar{B}_{(s)}$ mixing. An exploratory lattice NRQCD study with the one-loop matching in the infinitely heavy quark mass limit is found in Ref. [24]. We reanalyze the data in that work with the renormalization constant containing the finite heavy quark mass effect. We find that our new analysis resulted in a change of the value of the bag parameter, but it remains within the expected size of the error in the previous analysis as is also the case for B_B.

This paper is organized as follows. We summarize the definition of the lattice NRQCD action in Sec. II, and the heavy-light four-quark operators in Sec. III. Section IV is the main part of this paper, where we present the results of the one-loop matching calculations for bilinear operators (Sec.

IV A) and for the four-quark operators (Sec. IV B). The re-analysis of our previous NRQCD simulations are given in Sec. V. Section VI is devoted to our conclusion. Details of the one-loop calculations are collected in Appendices. The Feynman rules for the lattice NRQCD action is given in Appendix A, while several expressions of one-loop integrals and amplitudes are summarized in Appendix B and C, respectively.

II. LATTICE FORMULATION OF NRQCD

In this section we briefly summarize the definition of the NRQCD action used in the following perturbative calculations. A complete formulation of the lattice NRQCD is found in Ref. [13].

Our NRQCD action is defined by

$$S_{\mathrm{NRQCD}} = \sum_{x,y} Q^\dagger(x)(1-K_Q)(x,y)Q(y)$$
$$+ \sum_{x,y} \chi^\dagger(x)(1-K_\chi)(x,y)\chi(y). \quad (2.1)$$

The nonrelativistic two-component spinor fields Q and χ represent a heavy quark and an anti-quark, respectively. Their evolution is described by[1]

$$K_Q(x,y) = \left[\left(1-\frac{aH_0}{2n}\right)^n \left(1-\frac{a\,\delta H}{2}\right) \delta_4^{(-)} U_4^\dagger \left(1-\frac{a\,\delta H}{2}\right) \right.$$
$$\left. \times \left(1-\frac{aH_0}{2n}\right)^n \right](x,y), \quad (2.2)$$

$$K_\chi(x,y) = \left[\left(1-\frac{aH_0}{2n}\right)^n \left(1-\frac{a\,\delta H}{2}\right) \delta_4^{(+)} U_4 \left(1-\frac{a\,\delta H}{2}\right) \right.$$
$$\left. \times \left(1-\frac{aH_0}{2n}\right)^n \right](x,y), \quad (2.3)$$

where n denotes a stabilization parameter introduced in order to remove an instability arising from unphysical momentum modes in the evolution equation. Note that, following Ref. [13], all the link variable U_μ in the NRQCD action is always divided by the mean field value u_0 determined from the plaquette expectation value. This tadpole improvement will give rise to an $\mathcal{O}(g^2)$ counter term in the Feynman rule.

The operator $\delta_4^{(\pm)}$ is defined as $\delta_4^{(\pm)}(x,y) \equiv \delta_{x_4 \pm 1, y_4} \delta_{\mathbf{x},\mathbf{y}}$, and the Hamiltonians H_0 and δH are

$$H_0 = -\frac{\mathbf{\Delta}^{(2)}}{2aM_0}, \quad (2.4)$$

$$\delta H = -c_B \frac{g}{2aM_0} \sigma \cdot \mathbf{B}, \quad (2.5)$$

where aM_0 denotes a bare heavy quark mass in lattice unit. The operator $\mathbf{\Delta}^{(2)} \equiv \Sigma_{i=1}^3 \Delta_i^{(2)}$ is a Laplacian defined on the lattice through $\Delta_i^{(2)}$, the second symmetric covariant differentiation operator in the spatial direction i. The space-time indices x and y are implicit in these expressions. The Hamiltonian δH represents the effect of the spin-(chromo)magnetic interaction, in which $\mathbf{B}$ is the chromomagnetic field defined as a standard clover-leaf operator. g is a gauge coupling, and c_B is a constant to parametrize the strength of the $\sigma \cdot \mathbf{B}$ interaction. It should be tuned until the NRQCD action reproduces the same dynamics as that of continuum relativistic action. We take the tree level value $c_B = 1$. The relativistic four-component Dirac spinor field b is related to the two-component nonrelativistic field Q and χ appearing in the NRQCD action in Eq. (2.1) via the Foldy–Wouthuysen–Tani (FWT) transformation

$$b(x) = \sum_z R(x,z) \begin{pmatrix} Q(z) \\ \chi^\dagger(z) \end{pmatrix}, \quad (2.6)$$

where R is defined as

$$R = 1 - \frac{\gamma \cdot \mathbf{\Delta}^{(\pm)}}{2aM_0}, \quad (2.7)$$

where $\Delta_i^{(\pm)}$ is the first symmetric covariant differentiation operator in spatial direction.

The Feynman rules derived from the NRQCD action in Eq. (2.1) and the FWT transformation (2.6) are given in Appendix A. The light quark action is the $\mathcal{O}(a)$-improved Wilson action [27], and the gluon action is the standard plaquette action. The Feynman rules for light quarks and gluons are also summarized in Appendix A.

III. OPERATORS

The B parameters $B_L{}^2$ and B_S are defined using the $\Delta B = 2$ four-quark operators $\bar{b}\gamma_\mu(1-\gamma_5)q\bar{b}\gamma_\mu(1-\gamma_5)q$ and $\bar{b}(1-\gamma_5)q\bar{b}(1-\gamma_5)q$, respectively. In the perturbative matching, however, we have to consider other operators which mix under the radiative correction. Since the lattice regularization violates the chiral symmetry, some operators that do not appear in the matching between continuum regularizations are also necessary. We define the following set of operators:

---

[1] The evolution equations (2.2) and (2.3) are slightly different from the definition used, for example, in Ref. [26], where the $(1 - aH_0/2n)^n$ terms appear inside of the $(1 - a\,\delta H/2)$ terms.

[2] We use a notation B_L instead of the usual B_B in order to emphasize that it represents a matrix element of the ''LL'' operator.

$$O_{VLL} = \bar{b}\gamma_\mu P_L q \bar{b}\gamma_\mu P_L q, \tag{3.1}$$

$$O_{VRR} = \bar{b}\gamma_\mu P_R q \bar{b}\gamma_\mu P_R q, \tag{3.2}$$

$$O_{VLR} = \bar{b}\gamma_\mu P_L q \bar{b}\gamma_\mu P_R q, \tag{3.3}$$

$$O_{SLL} = \bar{b}P_L q \bar{b}P_L q, \tag{3.4}$$

$$O_{SLR} = \bar{b}P_L q \bar{b}P_R q, \tag{3.5}$$

$$\tilde{O}_{VLL} = \bar{b}\gamma_\mu P_L T^a q \bar{b}\gamma_\mu P_L T^a q, \tag{3.6}$$

$$\tilde{O}_{VRR} = \bar{b}\gamma_\mu P_R T^a q \bar{b}\gamma_\mu P_R T^a q, \tag{3.7}$$

$$\tilde{O}_{VLR} = \bar{b}\gamma_\mu P_L T^a q \bar{b}\gamma_\mu P_R T^a q, \tag{3.8}$$

$$\tilde{O}_{SLL} = \bar{b}P_L T^a q \bar{b}P_L T^a q, \tag{3.9}$$

$$\tilde{O}_{SLR} = \bar{b}P_L T^a q \bar{b}P_R T^a q, \tag{3.10}$$

where P_L and P_R are chirality projection operators $P_{L/R} = (1 \mp \gamma_5)/2$, and T^a is a generator of the SU(N) group. The operators with a tilde contains a summation over the SU(N) generators T^a. Fierz identities relate the 'tilde' operators in Eqs. (3.6)–(3.10) to those without tilde in Eqs. (3.1)–(3.5) as

$$\tilde{O}_{VLL} = \frac{N-1}{2N} O_{VLL}, \tag{3.11}$$

$$\tilde{O}_{VRR} = \frac{N-1}{2N} O_{VRR}, \tag{3.12}$$

$$\tilde{O}_{VLR} = -\frac{1}{2N} O_{VLR} - O_{SLR}, \tag{3.13}$$

$$\tilde{O}_{SLL} = -\frac{N+1}{2N} O_{SLL} - \frac{1}{4} O_{VLL}, \tag{3.14}$$

$$\tilde{O}_{SLR} = -\frac{1}{2N} O_{SLR} - \frac{1}{4} O_{VLR}. \tag{3.15}$$

We use these relations to eliminate the ''tilde'' operators from matching relations. We note that all equations except Eq. (3.14) are exact, whereas Eq. (3.14) is valid up to $\mathcal{O}(p/M_0)$ correction terms described by dimension seven operators. When computing the matching of O_{VLL} and O_{SLL} operators, the neglected terms give errors of $\mathcal{O}(\alpha_s p/M_0)$ through one-loop mixing.

In Sec. V we present our final result using the following set of operators in more conventional definitions:

$$O_L = \bar{b}\gamma_\mu(1-\gamma_5)q \bar{b}\gamma_\mu(1-\gamma_5)q, \tag{3.16}$$

$$O_R = \bar{b}\gamma_\mu(1+\gamma_5)q \bar{b}\gamma_\mu(1+\gamma_5)q, \tag{3.17}$$

$$O_S = \bar{b}(1-\gamma_5)q \bar{b}(1-\gamma_5)q, \tag{3.18}$$

$$O_N = 2\bar{b}\gamma_\mu(1-\gamma_5)q \bar{b}\gamma_\mu(1+\gamma_5)q$$
$$+ 4\bar{b}(1-\gamma_5)q \bar{b}(1+\gamma_5)q, \tag{3.19}$$

$$O_M = 2\bar{b}\gamma_\mu(1-\gamma_5)q \bar{b}\gamma_\mu(1+\gamma_5)q$$
$$- 4\bar{b}(1-\gamma_5)q \bar{b}(1+\gamma_5)q, \tag{3.20}$$

$$\tilde{O}_S = \bar{b}^i(1-\gamma_5)q^j \bar{b}^j(1-\gamma_5)q^i, \tag{3.21}$$

$$O_P = 2\bar{b}\gamma_\mu(1-\gamma_5)q \bar{b}\gamma_\mu(1+\gamma_5)q$$
$$+ 4N\bar{b}(1-\gamma_5)q \bar{b}(1+\gamma_5)q, \tag{3.22}$$

$$O_Q = 2N\bar{b}\gamma_\mu(1-\gamma_5)q \bar{b}\gamma_\mu(1+\gamma_5)q$$
$$+ 4\bar{b}(1-\gamma_5)q \bar{b}(1+\gamma_5)q, \tag{3.23}$$

$$O_T = (2+N)\bar{b}\gamma_\mu(1-\gamma_5)q \bar{b}\gamma_\mu(1+\gamma_5)q$$
$$- 2(3N^2-2N-4)\bar{b}(1-\gamma_5)q \bar{b}(1+\gamma_5)q. \tag{3.24}$$

The indices i and j, which appear in the definition of $\tilde{O}_S$, run over color of quarks, while other operators are products of color-singlet bilinear operators. As is obvious from Eqs. (3.1)–(3.24), the set of operators in conventional definition are related to the first set of operators as

$$O_L = 4O_{VLL}, \tag{3.25}$$

$$O_R = 4O_{VRR}, \tag{3.26}$$

$$O_S = 4O_{SLL}, \tag{3.27}$$

$$O_N = 8(O_{VLR} + 2O_{SLR}), \tag{3.28}$$

$$O_M = 8(O_{VLR} - 2O_{SLR}), \tag{3.29}$$

$$\tilde{O}_S = 8\left(\tilde{O}_{SLL} + \frac{1}{2N} O_{SLL}\right), \tag{3.30}$$

$$O_P = 8(O_{VLR} + 2NO_{SLR}), \tag{3.31}$$

$$O_Q = 8(NO_{VLR} + 2O_{SLR}), \tag{3.32}$$

$$O_T = 4(2+N)O_{VLR} - 8(3N^2 - 2N - 4)O_{SLR}. \tag{3.33}$$

IV. ONE-LOOP CALCULATION

In order to match the operators defined in the continuum theory, say the modified minimal subtraction $\overline{\text{MS}}$ scheme with the dimensional regularization, to the lattice counterparts, we compute the on-shell amplitude both in the continuum and on the lattice at one-loop level.

Let $O_X^{\overline{\text{MS}}}(\mu)$ and $O_X^{lat}(1/a)$ be certain continuum and lattice operators defined at scale μ and $1/a$, respectively. The on-shell amplitude for a certain external state can be expressed by a linear combination of tree-level amplitudes

$\langle O_Y \rangle_0$, where the subscript Y runs over all possible operators which can mix with $O_X^{\overline{MS}}$ and O_X^{lat} at one-loop: namely,

$$\langle O_X^{\overline{MS}}(\mu) \rangle = \langle O_X \rangle_0 + \frac{\alpha_s}{4\pi} \sum_Y \rho_{X,Y}^{\overline{MS}}(\mu) \langle O_Y \rangle_0 + \mathcal{O}(\alpha_s^2),$$

$$(4.1)$$

$$\langle O_X^{lat}(1/a) \rangle = \langle O_X \rangle_0 + \frac{\alpha_s}{4\pi} \sum_Y \rho_{X,Y}^{lat}(1/a) \langle O_Y \rangle_0 + \mathcal{O}(\alpha_s^2),$$

$$(4.2)$$

where $\alpha_s = g^2/4\pi$, and $\rho_{X,Y}^{\overline{MS}}(\mu)$ and $\rho_{X,Y}^{lat}(1/a)$ represent the one-loop coefficients in the $\overline{MS}$ and the lattice schemes. We take zero spatial momentum on-shell free quarks for the external state. This choice is the easiest and sufficient to obtain the matching coefficients uniquely, since we restrict ourselves to the matching at lowest operator dimension, for which no derivative operator appears.

Requiring that the both operators give identical one-loop on-shell amplitudes, we obtain the following matching relation:

$$O_X^{\overline{MS}}(\mu) = \sum_Y \left[\delta_{X,Y} + \frac{\alpha_s}{4\pi} (\rho_{X,Y}^{\overline{MS}}(\mu) - \rho_{X,Y}^{lat}(1/a)) \right.$$

$$\left. + \mathcal{O}(\alpha_s^2) \right] O_Y^{lat}(1/a). \qquad (4.3)$$

In the following we compute the coefficients $\rho_{X,Y}^{\overline{MS}}(\mu)$ and $\rho_{X,Y}^{lat}(1/a)$ for the heavy-light bilinear operators and $\Delta B = 2$ four-quark operators.

A. Bilinear operators

First of all, we give the expression for the matching of the bilinear operators for completeness. Although the one-loop coefficients for the matching of the heavy-light vector and axial vector currents have already been obtained by Morningstar and Shigemitsu [28] even through $\mathcal{O}(\alpha p/M_0)$ and $\mathcal{O}(\alpha a p)$, we present the one-loop matching coefficients for the general heavy-light bilinear operators for completeness.

The one-loop expression of the perturbative on-shell amplitudes of the heavy-light bilinear operator $\bar{b}\Gamma q$ with arbitrary Dirac structure Γ is given as

$$\langle (\bar{b}\Gamma q)(\mu) \rangle = \left[1 + \frac{\alpha_s}{4\pi} \rho_\Gamma(\mu) + \mathcal{O}(\alpha_s^2) \right] \langle \bar{b}\Gamma q \rangle_0, \quad (4.4)$$

for both continuum and lattice operators. There is no operator mixing in the lowest dimension bilinear operators. In the continuum (the $\overline{MS}$ scheme with totally anticommuting γ_5), the coefficient $\rho_\Gamma^{\overline{MS}}(\mu)$ is obtained [7,10,11] as

$$\rho_\Gamma^{\overline{MS}}(\mu) = C_F \left[\frac{H^2 - 4}{4} \ln\frac{\mu^2}{M_0^2} - \frac{3}{2} \ln\frac{\lambda^2}{M_0^2} + \frac{3H^2}{4} \right.$$

$$\left. - HH' - \frac{GH}{2} - \frac{11}{4} \right], \qquad (4.5)$$

TABLE I. Wave function renormalization constants for the NRQCD heavy quark.

aM_0	n	C_h
12.0	2	2.94(12)
10.0	2	2.63(7)
7.0	2	1.86(5)
6.5	2	1.67(12)
5.0	2	0.89(13)
4.5	2	0.52(12)
4.0	2	0.07(11)
3.8	2	$-0.13(12)$
3.5	2	$-0.49(11)$
3.0	2	$-1.20(9)$
2.6	2	$-1.93(8)$
2.1	3	$-2.97(8)$
1.5	3	$-5.10(6)$
1.3	3	$-6.10(6)$
1.2	3	$-6.67(6)$
0.9	4	$-8.68(5)$

where $C_F = (N^2 - 1)/2N$, and λ denotes a gluon mass introduced to regularize the infrared divergence. The constants H, H', and G are defined through the following equations,

$$H\Gamma \equiv \sum_{\mu=1}^D \gamma_\mu \Gamma \gamma_\mu, \quad H' \equiv \frac{dH}{dD}, \quad G\Gamma \equiv \gamma_4 \Gamma \gamma_4,$$

$$(4.6)$$

with space-time dimension $D = 4$. The corresponding one-loop expression for the lattice operator is

$$\rho_\Gamma^{lat}(1/a) = C_F [-\tfrac{3}{2} \ln(a^2\lambda^2) + \tfrac{1}{2}(C_l + C_h)$$

$$+ (4\pi)^2 [I_A + G I_B + (H - G)^2 I_C$$

$$+ (H - G)(I_D + I_F) + (H - G) G I_E]]. \qquad (4.7)$$

The infrared divergence of form $\tfrac{3}{2} C_F \ln\lambda^2$ is canceled between continuum and lattice expressions for any bilinear operator in the combination of the matching coefficient $\rho_\Gamma^{\overline{MS}} - \rho_\Gamma^{lat}$. The numerical value of the light quark wave function renormalization factor C_l is 9.076 for the $\mathcal{O}(a)$-improved action. If one uses the normalization $1/\sqrt{u_0}$ for the light quark field motivated by the tadpole improvement [12], the number becomes -0.164 for $u_0 \equiv \langle \tfrac{1}{3} \text{Tr} U_P \rangle^{1/4}$ (average plaquette), or 1.7106 for $u_0 \equiv 1/8\kappa_{crit}$ (critical hopping parameter). The heavy quark wave function renormalization C_h depends on the heavy quark mass aM_0, and its numerical values are summarized in Table I. The constants I_A, I_B, I_C, I_D, I_E, and I_F are one-loop integrals from the vertex corrections shown in Fig. 1. Their explicit expressions are given in Appendix B [Eqs. (B1)–(B6)], and their numerical values are given in Table II.

In the following, we present the expressions of the matching factors for the temporal component of the axial current A_4 and for the pseudoscalar density P.
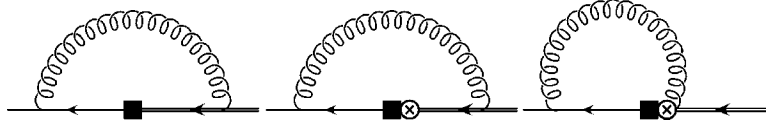
FIG. 1. Vertex correction for the bilinear operator.

1. Axial vector current

For the axial-vector current A_4 with $\Gamma = \gamma_5 \gamma_4$, we obtain $H = 2$, $H' = 1$, and $G = -1$, for which the matching coefficients are

$$\rho_{A_4}^{\overline{\text{MS}}} = C_F \left[-\frac{3}{2} \ln \frac{\lambda^2}{M_0^2} - \frac{3}{4} \right], \tag{4.8}$$

$$\rho_{A_4}^{lat}(1/a) = C_F [-\tfrac{3}{2} \ln(a^2 \lambda^2) + \tfrac{1}{2}(C_h + C_l)$$
$$+ (4\pi)^2 (I_A - I_B + 9 I_C + 3 I_D - 3 I_E + 3 I_F)]. \tag{4.9}$$

$\rho_{A_4}^{\overline{\text{MS}}}$ does not have the logarithmic scale dependence because of the (partial-)conservation of the axial vector current. Combining the two expressions we obtain the matching relation

$$A_4^{\overline{\text{MS}}} = \left[1 + \frac{\alpha_s}{4\pi} (2 \ln(a^2 M_0^2) + \zeta_A) + \mathcal{O}(\alpha_s^2) \right] A_4^{lat}(1/a), \tag{4.10}$$

where

$$\zeta_A = C_F [-\tfrac{3}{4} - \tfrac{1}{2}(C_h + C_l)$$
$$- (4\pi)^2 (I_A - I_B + 9 I_C + 3 I_D - 3 I_E + 3 I_F)]. \tag{4.11}$$

Numerical values of the coefficient ζ_A are listed in Table III.

2. Pseudoscalar density

For the pseudo-scalar density P with $\Gamma = \gamma_5$, we obtain $H = -4$, $H' = -1$, and $G = -1$. The matching coefficients are

$$\rho_P^{\overline{\text{MS}}}(\mu) = C_F \left[3 \ln \frac{\mu^2}{M_0^2} - \frac{3}{2} \ln \frac{\lambda^2}{M_0^2} + \frac{13}{4} \right], \tag{4.12}$$

$$\rho_P^{lat}(1/a) = C_F [-\tfrac{3}{2} \ln(a^2 \lambda^2) + \tfrac{1}{2}(C_h + C_l)$$
$$+ (4\pi)^2 (I_A - I_B + 9 I_C - 3 I_D + 3 I_E - 3 I_F)]. \tag{4.13}$$

Combining these expressions we obtain the matching relation

$$P^{\overline{\text{MS}}}(\mu) = \left[1 + \frac{\alpha_s}{4\pi} \left(4 \ln \frac{\mu^2}{M_0^2} + 2 \ln(a^2 M_0^2) + \zeta_P \right) \right.$$
$$\left. + \mathcal{O}(\alpha_s^2) \right] P^{lat}(1/a), \tag{4.14}$$

where

$$\zeta_P = C_F [\tfrac{13}{4} - \tfrac{1}{2}(C_h + C_l)$$
$$- (4\pi)^2 (I_A - I_B + 9 I_C - 3 I_D + 3 I_E - 3 I_F)]. \tag{4.15}$$

Numerical values of the coefficient ζ_P are listed in Table III.

TABLE II. Integrals I_A, I_B, I_C, I_D, I_E, and I_F.

aM_0	n	I_A	I_B	I_C	I_D	I_E	I_F
12.0	2	0.030932(15)	−0.016562(9)	0.000794(1)	−0.000029(0)	0.001020(1)	−0.000519(0)
10.0	2	0.030277(15)	−0.016041(8)	0.000936(1)	−0.000031(0)	0.001209(1)	−0.000623(0)
7.0	2	0.028754(14)	−0.014812(8)	0.001282(1)	−0.000032(0)	0.001678(2)	−0.000890(0)
6.5	2	0.028388(14)	−0.014512(8)	0.001367(1)	−0.000031(0)	0.001791(2)	−0.000958(0)
5.0	2	0.026993(13)	−0.013325(7)	0.001702(2)	−0.000024(0)	0.002256(2)	−0.001246(0)
4.5	2	0.026371(13)	−0.012802(7)	0.001853(2)	−0.000019(0)	0.002469(2)	−0.001384(0)
4.0	2	0.025697(24)	−0.012179(7)	0.002033(2)	−0.000010(0)	0.002723(3)	−0.001557(0)
3.8	2	0.025327(12)	−0.011894(6)	0.002116(2)	−0.000006(0)	0.002843(3)	−0.001639(0)
3.5	2	0.024791(12)	−0.011422(6)	0.002252(2)	0.000003(0)	0.003039(3)	−0.001780(0)
3.0	2	0.023692(12)	−0.010492(5)	0.002524(2)	0.000025(0)	0.003423(3)	−0.002076(0)
2.6	2	0.022733(23)	−0.009579(5)	0.002793(3)	0.000052(0)	0.003826(4)	−0.002396(0)
2.1	3	0.021122(11)	−0.008532(5)	0.003253(3)	0.000111(0)	0.004524(4)	−0.002966(1)
1.5	3	0.018483(9)	−0.006337(3)	0.003995(4)	0.000252(0)	0.005707(6)	−0.004153(1)
1.3	3	0.017439(9)	−0.005419(3)	0.004320(4)	0.000331(0)	0.006230(5)	−0.004792(1)
1.2	3	0.016842(17)	−0.004921(3)	0.004502(4)	0.000381(0)	0.006529(6)	−0.005191(1)
0.9	4	0.014482(17)	−0.003598(2)	0.005228(5)	0.000609(0)	0.007825(7)	−0.006921(1)

TABLE III. Matching coefficients $\zeta_{A,P}$ for A_4, P.

aM_0	n	ζ_A	ζ_P
12.0	2	$-14.59(8)$	$-11.26(8)$
10.0	2	$-14.23(5)$	$-11.26(5)$
7.0	2	$-13.33(3)$	$-11.29(3)$
6.5	2	$-13.11(8)$	$-11.30(8)$
5.0	2	$-12.21(9)$	$-11.34(9)$
4.5	2	$-11.79(8)$	$-11.36(8)$
4.0	2	$-11.28(7)$	$-11.40(7)$
3.8	2	$-11.05(8)$	$-11.40(8)$
3.5	2	$-10.66(7)$	$-11.42(7)$
3.0	2	$-9.86(6)$	$-11.45(6)$
2.6	2	$-9.04(5)$	$-11.51(5)$
2.1	3	$-7.89(5)$	$-11.89(5)$
1.5	3	$-5.47(4)$	$-12.27(4)$
1.3	3	$-4.31(4)$	$-12.49(4)$
1.2	3	$-3.63(4)$	$-12.67(4)$
0.9	4	$-1.14(3)$	$-13.66(3)$

B. Four-quark operators

We present the one-loop matching calculation of the four-quark operators O_{VLL} and O_{SLL}, which appear in the evaluation of the mass and width differences in the $B_{d(s)}$-$\bar{B}_{d(s)}$ systems.

1. O_{VLL}

In the continuum theory preserving the chiral symmetry, the four-quark operator O_{VLL} mixes with O_{SLL} under the radiative correction. At the one-loop level, the on-shell amplitude of $O_{VLL}(\mu)$ defined at scale μ is written as

$$\langle O_{VLL}^{\overline{MS}}(\mu)\rangle = \left[1 + \frac{\alpha_s}{4\pi}\rho_{VLL,VLL}^{\overline{MS}}(\mu)\right]\langle O_{VLL}\rangle_0$$
$$+ \left[\frac{\alpha_s}{4\pi}\rho_{VLL,SLL}^{\overline{MS}}\right]\langle O_{SLL}\rangle_0, \qquad (4.16)$$

where

$$\rho_{VLL,VLL}^{\overline{MS}}(\mu) = 2\ln\frac{M_0^2}{\mu^2} - 4\ln\frac{\lambda^2}{M_0^2} - \frac{35}{3}, \qquad (4.17)$$

$$\rho_{VLL,SLL}^{\overline{MS}} = -8. \qquad (4.18)$$

The mixing coefficient $\rho_{VLL,SLL}^{\overline{MS}}$ does not have the scale dependence at the one-loop level.

The same operator mixes with four operators O_{VLR}, O_{SLR}, O_{SLL}, and O_{VRR} on the lattice due to the lack of the chiral symmetry. We obtain the following expression for the on-shell amplitude of the lattice operator $O_{VLL}(1/a)$:
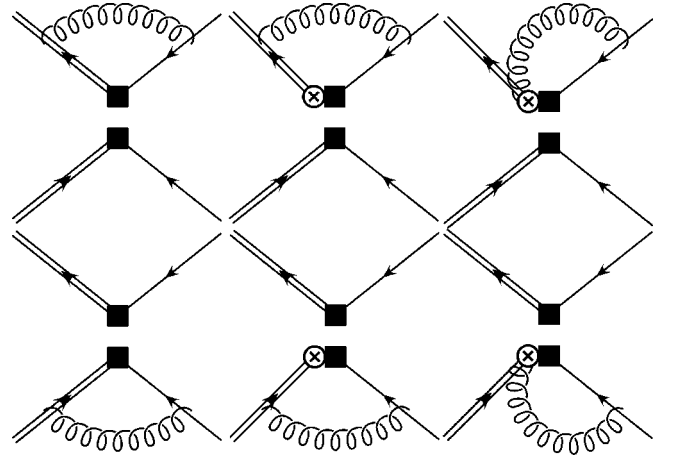

FIG. 2. Heavy-light vertex corrections in color singlet channel.

$$\langle O_{VLL}^{lat}(1/a)\rangle = \left[1 + \frac{\alpha_s}{4\pi}\rho_{VLL,VLL}^{lat}(1/a)\right]\langle O_{VLL}\rangle_0$$
$$+ \left[\frac{\alpha_s}{4\pi}\rho_{VLL,VLR}^{lat}\right]\langle O_{VLR}\rangle_0 + \left[\frac{\alpha_s}{4\pi}\rho_{VLL,SLR}^{lat}\right]$$
$$\times\langle O_{SLR}\rangle_0 + \left[\frac{\alpha_s}{4\pi}\rho_{VLL,SLL}^{lat}\right]\langle O_{SLL}\rangle_0$$
$$+ \left[\frac{\alpha_s}{4\pi}\rho_{VLL,VRR}^{lat}\right]\langle O_{VRR}\rangle_0, \qquad (4.19)$$

where

$$\rho_{VLL,VLL}^{lat}(1/a) = -4\ln(a^2\lambda^2) + C_F[C_l + C_h]$$
$$+ (4\pi)^2[\tfrac{10}{3}I_A + 2I_C + 4I_E + \tfrac{1}{3}(I_G - 3$$
$$\times(I_H + I_I + I_J + 2I_K) + 16I_L + I_N)], \qquad (4.20)$$

$$\rho_{VLL,VLR}^{lat} = (4\pi)^2[2(-2I_B - \tfrac{5}{3}(I_D + I_F))], \qquad (4.21)$$

$$\rho_{VLL,SLR}^{lat} = (4\pi)^2[2(-4I_B + \tfrac{10}{3}(I_D + I_F))], \qquad (4.22)$$

$$\rho_{VLL,SLL}^{lat} = (4\pi)^2[-16(2I_C - I_E)], \qquad (4.23)$$

$$\rho_{VLL,VRR}^{lat} = (4\pi)^2\left[-\frac{4}{3}I_M\right]. \qquad (4.24)$$

The integrals I_A, I_B, I_C, I_D, I_E, and I_F come from the diagrams in which a gluon mediates between heavy and light quark lines as shown in Figs. 2 and 3. These are the same integrals as in the vertex correction of the bilinear operators, whose numerical values are given in Table II. Other integrals I_G, I_H, I_I, I_J, I_K, I_L, I_M, and I_N are characteristic of the corrections of the four-quark operators. The diagrams in which a gluon line mediates between two heavy quark lines (Fig. 4) produce the five integrals I_G, I_H, I_I, I_J, and I_K, whose expressions are given in Appendix B [Eqs. (B7)–(B11)]. Their heavy quark mass dependence is summarized

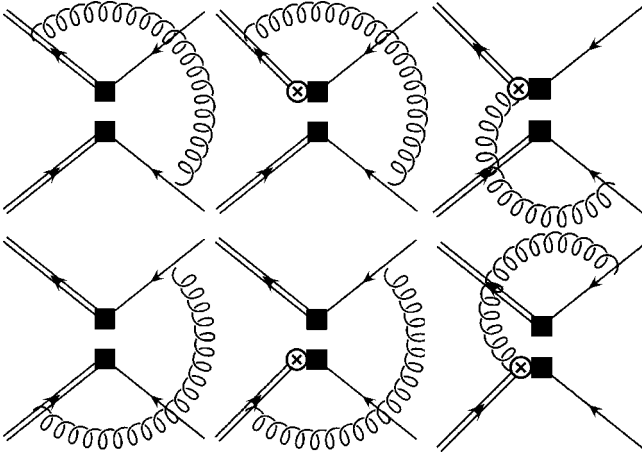FIG. 3. Heavy-light vertex corrections in color octet channel.

FIG. 4. Heavy-heavy vertex corrections in color octet channel.

in Table IV. Three others, I_L, I_M, and I_N defined in Eqs. (B12)–(B14), correspond to the diagrams in which the two light quark lines (Fig. 5) are connected by a gluon line. These do not depend on the heavy quark mass, and their numerical values are

$$I_L = -0.004\,635(3), \quad I_M = -0.002\,433(1),$$

$$\text{(4.25)}$$

$$I_N = -0.012\,204(6).$$

In Appendix C, one-loop expressions of the lattice on-shell amplitudes with general four-quark operators $\bar{b}\Gamma q\bar{b}\Gamma q$ are presented. The above result in Eq. (4.19) is obtained by applying the Fierz transformation for the color and spinor indices on the expressions (C4)–(C7).

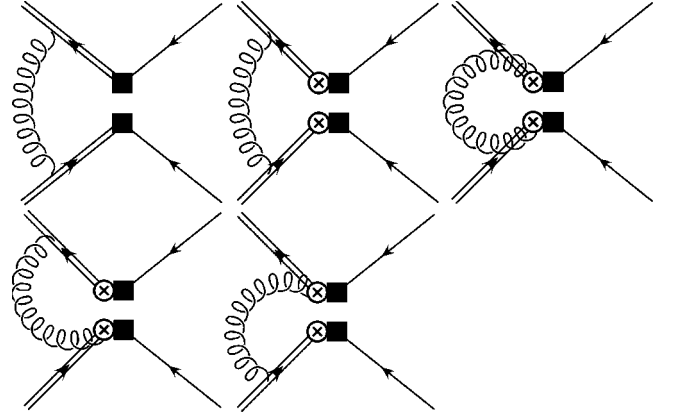Combining the continuum and the lattice results we obtain

$$O_{VLL}^{\overline{MS}}(\mu) = \left[1 + \frac{\alpha_s}{4\pi}(\rho_{VLL,VLL}^{\overline{MS}}(\mu) \right.$$

$$\left. - \rho_{VLL,VLL}^{lat}(1/a)) \right] O_{VLL}^{lat}(1/a)$$

$$+ \left[-\frac{\alpha_s}{4\pi}\rho_{VLL,VLR}^{lat} \right] O_{VLR}^{lat}(1/a)$$

$$+ \left[-\frac{\alpha_s}{4\pi}\rho_{VLL,SLR}^{lat} \right] O_{SLR}^{lat}(1/a)$$

$$+ \left[\frac{\alpha_s}{4\pi}(\rho_{VLL,SLL}^{\overline{MS}} - \rho_{VLL,SLL}^{lat}) \right] O_{SLL}^{lat}(1/a)$$

$$+ \left[-\frac{\alpha_s}{4\pi}\rho_{VLL,VRR}^{lat} \right] O_{VRR}^{lat}(1/a). \quad \text{(4.26)}$$

The numerical values of $\rho_{VLL,Y}^{lat}$ are listed in Tables V.

The matching relation for O_L is obtained using the conversion formula (3.25)–(3.32) as follows:

TABLE IV. Integrals I_G, I_H, I_I, I_J, and I_K for $c_{sw} = 1$.

aM_0	n	I_G	I_H	I_I	I_J	I_K
12.0	2	0.01858(8)	0.000075(0)	0.000029(0)	−0.000160(0)	0.000008(0)
10.0	2	0.01674(7)	0.000104(0)	0.000041(0)	−0.000231(0)	0.000013(0)
7.0	2	0.01223(5)	0.000193(1)	0.000073(0)	−0.000471(0)	0.000037(0)
6.5	2	0.01107(5)	0.000220(1)	0.000081(0)	−0.000547(0)	0.000045(0)
5.0	2	0.00653(3)	0.000338(1)	0.000118(0)	−0.000924(0)	0.000095(0)
4.5	2	0.00439(2)	0.000400(2)	0.000134(1)	−0.001140(0)	0.000127(0)
4.0	2	0.00183(2)	0.000474(0)	0.000153(0)	−0.001443(0)	0.000176(0)
3.8	2	0.00063(2)	0.000515(2)	0.000160(1)	−0.001599(0)	0.000203(0)
3.5	2	−0.00138(1)	0.000580(2)	0.000171(1)	−0.001885(0)	0.000254(0)
3.0	2	−0.00545(2)	0.000718(3)	0.000185(1)	−0.002566(1)	0.000385(0)
2.6	2	−0.00964(2)	0.000862(1)	0.000182(0)	−0.003416(1)	0.000563(0)
2.1	3	−0.01528(5)	0.001154(5)	0.000146(1)	−0.005237(1)	0.000977(1)
1.5	3	−0.02721(9)	0.001680(5)	−0.000234(1)	−0.010264(3)	0.002270(1)
1.3	3	−0.03274(9)	0.001932(8)	−0.000613(2)	−0.013665(4)	0.003201(2)
1.2	3	−0.03592(4)	0.002081(2)	−0.000926(2)	−0.016038(4)	0.003865(2)
0.9	4	−0.04662(12)	0.002760(9)	−0.002752(9)	−0.028512(8)	0.007507(4)

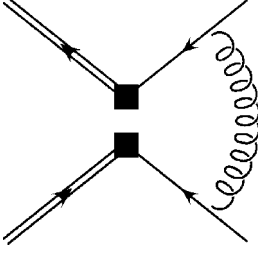FIG. 5. Light-light vertex correction in color octet channel.

$$O_L^{\overline{\mathrm{MS}}}(\mu) = \left[1 + \frac{\alpha_s}{4\pi}\left(-2\ln\frac{\mu^2}{M_0^2} + 4\ln(a^2 M_0^2) + \zeta_{L,L} \right) \right]$$

$$\times O_L^{lat}(1/a) + \frac{\alpha_s}{4\pi}\zeta_{L,S} O_S^{lat}(1/a)$$

$$+ \frac{\alpha_s}{4\pi}\zeta_{L,R} O_R^{lat}(1/a) + \frac{\alpha_s}{4\pi}\zeta_{L,N} O_N^{lat}(1/a)$$

$$+ \frac{\alpha_s}{4\pi}\zeta_{L,M} O_M^{lat}(1/a). \qquad (4.27)$$

The coefficients $\zeta_{L,S}$, $\zeta_{L,R}$, $\zeta_{L,N}$, and $\zeta_{L,M}$ are listed in Table VI. The coefficient $\zeta_{L,M}$ of O_M^{lat} vanishes in the static limit, and other coefficients agree with the previous work [14,9] in the same limit.

2. O_{SLL}

The matching relation for the operator O_{SLL} is obtained in a similar manner.

The operator O_{SLL} mixes with O_{VLL} with the radiative correction in the continuum. The on-shell amplitude with O_{SLL} for the zero momentum external state is written as

$$\langle O_{SLL}^{\overline{\mathrm{MS}}}(\mu) \rangle = \left[1 + \frac{\alpha_s}{4\pi}\rho_{SLL,SLL}^{\overline{\mathrm{MS}}}(\mu) \right] \langle O_{SLL} \rangle_0$$

$$+ \frac{\alpha_s}{4\pi}\rho_{SLL,VLL}^{\overline{\mathrm{MS}}}(\mu) \langle O_{VLL} \rangle_0, \qquad (4.28)$$

at the one-loop level. The coefficients are

$$\rho_{SLL,SLL}^{\overline{\mathrm{MS}}}(\mu) = \frac{16}{3}\ln\frac{\mu^2}{M_0^2} - \frac{4}{3}\ln\frac{\lambda^2}{M_0^2} + 10, \qquad (4.29)$$

$$\rho_{SLL,VLL}^{\overline{\mathrm{MS}}}(\mu) = \frac{1}{3}\ln\frac{\mu^2}{M_0^2} + \frac{2}{3}\ln\frac{\lambda^2}{M_0^2} + \frac{3}{2}. \qquad (4.30)$$

The lattice operator O_{SLL}^{lat} mixes with five operators in the on-shell amplitude as

$$\langle O_{SLL}^{lat} \rangle = \left[1 + \frac{\alpha_s}{4\pi}\rho_{SLL,SLL}^{lat}(1/a) \right] \langle O_{SLL} \rangle_0$$

$$+ \left[\frac{\alpha_s}{4\pi}\rho_{SLL,VLL}^{lat}(1/a) \right]\langle O_{VLL} \rangle_0 + \left[\frac{\alpha_s}{4\pi}\rho_{SLL,SLR}^{lat} \right]$$

$$\times \langle O_{SLR} \rangle_0 + \left[\frac{\alpha_s}{4\pi}\rho_{SLL,VLR}^{lat} \right]\langle O_{VLR} \rangle_0$$

$$+ \left[\frac{\alpha_s}{4\pi}\rho_{SLL,VRR}^{lat} \right]\langle O_{VRR} \rangle_0, \qquad (4.31)$$

where

TABLE V. Matching coefficients $O_{VLL,Y}^{lat}$ for $c_{sw} = 1$. The infrared divergence $-4\ln(a^2\lambda^2)$ is subtracted from $\rho_{VLL,VLL}^{lat}$. The tadpole improvement is applied such that the normalization of light quark field becomes $\sqrt{8\kappa_{crit}}$.

aM_0	n	$\rho_{VLL,VLL}^{lat}$	$\rho_{VLL,VLR}^{lat}$	$\rho_{VLL,SLR}^{lat}$	$\rho_{VLL,SLL}^{lat}$	$\rho_{VLL,VRR}^{lat}$
12.0	2	19.78(16)	10.751(2)	20.353(4)	−1.4375(4)	0.51217(9)
10.0	2	19.10(9)	10.480(2)	19.588(4)	−1.6789(4)	0.51217(9)
7.0	2	17.47(7)	9.840(2)	17.740(4)	−2.2483(5)	0.51217(9)
6.5	2	17.07(16)	9.687(2)	17.292(4)	−2.3830(5)	0.51217(9)
5.0	2	15.47(17)	9.091(2)	15.511(3)	−2.9032(6)	0.51217(9)
4.5	2	14.74(16)	8.828(2)	14.705(3)	−3.1306(7)	0.51217(9)
4.0	2	13.85(15)	8.519(2)	13.742(3)	−3.3948(7)	0.51217(9)
3.8	2	13.46(16)	8.381(2)	13.301(3)	−3.5138(8)	0.51217(9)
3.5	2	12.78(15)	8.153(2)	12.568(3)	−3.7104(8)	0.51217(9)
3.0	2	11.44(12)	7.710(2)	11.103(3)	−4.0868(9)	0.51217(9)
2.6	2	10.10(11)	7.286(2)	9.641(2)	−4.4438(9)	0.51217(9)
2.1	3	8.26(11)	6.894(1)	7.778(2)	−4.9772(10)	0.51217(9)
1.5	3	4.76(8)	6.059(2)	3.902(1)	−5.7882(12)	0.51217(9)
1.3	3	3.27(8)	5.773(2)	2.154(2)	−6.0962(13)	0.51217(9)
1.2	3	2.47(8)	5.642(2)	1.155(1)	−6.2536(13)	0.51217(9)
0.9	4	0.06(7)	5.596(1)	−2.098(1)	−6.6608(15)	0.51217(9)

TABLE VI. Matching coefficients ζ for O_{VLL}.

aM_0	n	ζ_{LL}	ζ_{LN}	ζ_{LM}	ζ_{LS}	ζ_{LR}
12.0	2	$-31.46(16)$	$-5.232(3)$	$-0.1441(0)$	$-6.572(2)$	$-0.51217(9)$
10.0	2	$-30.78(9)$	$-5.068(3)$	$-0.1720(1)$	$-6.326(2)$	$-0.51217(9)$
7.0	2	$-29.14(7)$	$-4.677(2)$	$-0.2426(1)$	$-5.755(2)$	$-0.51217(9)$
6.5	2	$-28.75(16)$	$-4.583(2)$	$-0.2604(1)$	$-5.623(2)$	$-0.51217(9)$
5.0	2	$-27.14(17)$	$-4.211(2)$	$-0.3343(1)$	$-5.105(2)$	$-0.51217(9)$
4.5	2	$-26.41(16)$	$-4.045(2)$	$-0.3693(1)$	$-4.878(1)$	$-0.51217(9)$
4.0	2	$-25.53(15)$	$-3.847(2)$	$-0.4126(1)$	$-4.613(2)$	$-0.51217(9)$
3.8	2	$-25.13(16)$	$-3.757(2)$	$-0.4330(1)$	$-4.494(2)$	$-0.51217(9)$
3.5	2	$-24.46(15)$	$-3.609(2)$	$-0.4676(1)$	$-4.299(2)$	$-0.51217(9)$
3.0	2	$-23.12(12)$	$-3.315(2)$	$-0.5400(2)$	$-3.923(2)$	$-0.51217(9)$
2.6	2	$-21.78(11)$	$-3.026(2)$	$-0.6169(2)$	$-3.564(2)$	$-0.51217(9)$
2.1	3	$-19.93(11)$	$-2.695(2)$	$-0.7515(2)$	$-3.029(2)$	$-0.51217(9)$
1.5	3	$-16.45(8)$	$-2.002(1)$	$-1.0267(3)$	$-2.221(2)$	$-0.51217(9)$
1.3	3	$-14.95(8)$	$-1.712(1)$	$-1.1739(3)$	$-1.913(2)$	$-0.51217(9)$
1.2	3	$-14.15(8)$	$-1.555(1)$	$-1.2660(3)$	$-1.756(2)$	$-0.51217(9)$
0.9	4	$-11.74(7)$	$-1.136(1)$	$-1.6612(4)$	$-1.351(3)$	$-0.51217(9)$

$$\rho_{SLL,SLL}^{lat}(1/a) = -\tfrac{4}{3}\ln(a^2\lambda^2) + C_F[C_l + C_h]$$
$$+ (4\pi)^2[\tfrac{1}{3}(4I_A + 52I_C + 20I_E - 2$$
$$\times(I_G + I_H + I_I + I_J + 2I_K + I_N))], \qquad (4.32)$$

$$\rho_{SLL,VLL}^{lat}(1/a) = \tfrac{2}{3}\ln(a^2\lambda^2) + (4\pi)^2[\tfrac{1}{12}(2(-3I_A - 7I_C + I_E)$$
$$- 3I_G + I_H + I_I + I_J + 2I_K - 16I_L - 3I_N)], \qquad (4.33)$$

$$\rho_{SLL,SLR}^{lat} = (4\pi)^2[2[\tfrac{3}{2}I_B + \tfrac{17}{6}(I_D + I_F)]], \qquad (4.34)$$

$$\rho_{SLL,VLR}^{lat} = (4\pi)^2[2[\tfrac{1}{4}I_B - \tfrac{5}{12}(I_D + I_F)]], \qquad (4.35)$$

$$\rho_{SLL,VRR}^{lat} = (4\pi)^2[\tfrac{1}{3}I_M], \qquad (4.36)$$

Numerical values of $\rho_{SLL,Y}^{lat}$ are given in Table VII.

Combining the continuum and the lattice results we obtain

TABLE VII. Matching coefficients $O_{SLL,Y}^{lat}$ for $c_{sw}=1$. The infrared divergences $-\tfrac{4}{3}\ln(a^2\lambda^2)$ and $\tfrac{2}{3}\ln(a^2\lambda^2)$ are subtracted from $\rho_{SLL,SLL}^{lat}$ and $\rho_{SLL,VLL}^{lat}$ respectively. The tadpole improvement is applied such that the normalization of light quark field becomes $\sqrt{8\kappa_{crit}}$.

aM	n	$\rho_{SLL,SLL}^{lat}$	$\rho_{SLL,VLL}^{lat}$	$\rho_{SLL,SLR}^{lat}$	$\rho_{SLL,VLR}^{lat}$	$\rho_{SLL,VRR}^{lat}$
12.0	2	15.26(16)	$-1.8396(16)$	$-8.3367(14)$	$-1.2359(3)$	$-0.12804(3)$
10.0	2	15.50(9)	$-1.7380(13)$	$-8.1851(13)$	$-1.1811(2)$	$-0.12804(3)$
7.0	2	16.09(7)	$-1.4903(9)$	$-7.8368(15)$	$-1.0479(3)$	$-0.12804(3)$
6.5	2	16.24(16)	$-1.4299(8)$	$-7.7565(15)$	$-1.0154(3)$	$-0.12804(3)$
5.0	2	16.81(17)	$-1.1879(6)$	$-7.4509(14)$	$-0.8857(2)$	$-0.12804(3)$
4.5	2	17.05(16)	$-1.0782(5)$	$-7.3204(13)$	$-0.8267(2)$	$-0.12804(3)$
4.0	2	17.35(15)	$-0.9466(5)$	$-7.1714(13)$	$-0.7557(2)$	$-0.12804(3)$
3.8	2	17.50(16)	$-0.8862(4)$	$-7.1061(13)$	$-0.7230(2)$	$-0.12804(3)$
3.5	2	17.71(15)	$-0.7852(4)$	$-7.0013(12)$	$-0.6684(2)$	$-0.12804(3)$
3.0	2	18.15(12)	$-0.5837(3)$	$-6.8068(11)$	$-0.5587(2)$	$-0.12804(3)$
2.6	2	18.59(11)	$-0.3823(3)$	$-6.6347(11)$	$-0.4481(1)$	$-0.12804(3)$
2.1	3	19.56(11)	$-0.1036(3)$	$-6.5966(10)$	$-0.2982(1)$	$-0.12804(3)$
1.5	3	20.93(8)	0.4334(2)	$-6.4940(10)$	0.0127(1)	$-0.12804(3)$
1.3	3	21.57(8)	0.6692(3)	$-6.5593(10)$	0.1589(1)	$-0.12804(3)$
1.2	3	21.96(8)	0.8006(3)	$-6.6362(10)$	0.2443(1)	$-0.12804(3)$
0.9	4	23.95(7)	1.2199(4)	$-7.3536(9)$	0.5465(1)	$-0.12804(3)$

TABLE VIII. Matching coefficients ζ for O_{SLL}.

aM_0	n	ζ_{SS}	ζ_{SL}	ζ_{SP}	ζ_{ST}	ζ_{SR}
12.0	2	−5.26(16)	3.3396(16)	0.65405(10)	−0.014414(1)	0.12804(3)
10.0	2	−5.50(9)	3.2380(13)	0.63362(10)	−0.017204(1)	0.12804(3)
7.0	2	−6.09(7)	2.9903(9)	0.58467(9)	−0.024260(2)	0.12804(3)
6.5	2	−6.24(16)	2.9299(8)	0.57291(9)	−0.026043(2)	0.12804(3)
5.0	2	−6.81(17)	2.6879(6)	0.52643(8)	−0.033428(2)	0.12804(3)
4.5	2	−7.05(16)	2.5782(5)	0.50564(8)	−0.036930(2)	0.12804(3)
4.0	2	−7.35(15)	2.4466(5)	0.48095(7)	−0.041261(3)	0.12804(3)
3.8	2	−7.50(16)	2.3862(4)	0.46972(7)	−0.043297(3)	0.12804(3)
3.5	2	−7.71(15)	2.2852(4)	0.45114(7)	−0.046764(3)	0.12804(3)
3.0	2	−8.16(12)	2.0837(3)	0.41443(6)	−0.054001(3)	0.12804(3)
2.6	2	−8.59(11)	1.8823(3)	0.37830(6)	−0.061688(4)	0.12804(3)
2.1	3	−9.56(11)	1.6036(3)	0.33695(5)	−0.075151(5)	0.12804(3)
1.5	3	−10.93(8)	1.0666(2)	0.25032(4)	−0.102676(7)	0.12804(3)
1.3	3	−11.57(8)	0.8308(3)	0.21406(4)	−0.117394(8)	0.12804(3)
1.2	3	−11.96(8)	0.6994(3)	0.19437(3)	−0.126601(9)	0.12804(3)
0.9	4	−13.95(7)	0.2801(4)	0.14209(3)	−0.166128(11)	0.12804(3)

$$O_{SLL}^{\overline{\text{MS}}}(\mu) = \left[1 + \frac{\alpha_s}{4\pi}(\rho_{SLL,SLL}^{\overline{\text{MS}}}(\mu) \right.$$

$$\left. - \rho_{SLL,SLL}^{lat}(1/a)) \right] O_{SLL}^{lat}(1/a)$$

$$+ \left[\frac{\alpha_s}{4\pi}(\rho_{SLL,VLL}^{\overline{\text{MS}}}(\mu) - \rho_{SLL,VLL}^{lat}(1/a)) \right]$$

$$\times O_{VLL}^{lat}(1/a) + \left[-\frac{\alpha_s}{4\pi}\rho_{SLL,SLR}^{lat} \right] O_{SLR}^{lat}(1/a)$$

$$+ \left[-\frac{\alpha_s}{4\pi}\rho_{SLL,VLR}^{lat} \right] O_{VLR}^{lat}(1/a)$$

$$+ \left[-\frac{\alpha_s}{4\pi}\rho_{SLL,VRR}^{lat} \right] O_{SLL,VRR}^{lat}(1/a). \quad (4.37)$$

The matching relation for O_S is obtained using the conversion formula (3.25)–(3.32) as follows:

$$O_S^{\overline{\text{MS}}}(\mu) = \left[1 + \frac{\alpha_s}{4\pi}\left(\frac{16}{3}\ln\frac{\mu^2}{M_0^2} + \frac{4}{3}\ln(a^2 M_0^2) + \zeta_{S,S} \right) \right]$$

$$\times O_S^{lat}(1/a) + \frac{\alpha_s}{4\pi}\left[\frac{1}{3}\ln\frac{\mu^2}{M_0^2} - \frac{2}{3}\ln(a^2 M_0^2) + \zeta_{S,L} \right]$$

$$\times O_L^{lat}(1/a) + \frac{\alpha_s}{4\pi}\zeta_{S,R}O_R^{lat}(1/a)$$

$$+ \frac{\alpha_s}{4\pi}\zeta_{S,P}O_P^{lat}(1/a) + \frac{\alpha_s}{4\pi}\zeta_{S,T}O_T^{lat}(1/a). \quad (4.38)$$

The coefficients $\zeta_{S,S}$, $\zeta_{S,L}$, $\zeta_{S,R}$, $\zeta_{S,P}$, and $\zeta_{S,T}$ are listed in Table VIII. The coefficient $\zeta_{S,T}$ of O_T^{lat} vanishes in the static limit, and other coefficients agree with the previous work [24,25] in the same limit.

V. PHYSICS RESULTS

Using the one-loop coefficients obtained in this work, we reanalyze the lattice NRQCD calculations of B_L [14] and of B_S [24]. These previous calculations were performed with the lattice NRQCD action for heavy quark, but the perturbative matching of the four-quark operators was done using the coefficients in the infinitely heavy quark mass limit. Due to this approximation for the matching coefficients, the previous results contain errors of order $\alpha_s/(aM)$, which is one of the largest uncertainties among all the systematic errors.

A. B_L

The B parameter B_L is defined through

$$B_L(\mu) \equiv \frac{\langle \bar{B}^0 | O_L^{\overline{\text{MS}}}(\mu) | B^0 \rangle}{\frac{8}{3}\langle \bar{B}^0 | A_4^{\overline{\text{MS}}} | 0 \rangle \langle 0 | A_4^{\overline{\text{MS}}} | B^0 \rangle}, \quad (5.1)$$

where the scale μ is usually set at the b quark mass M_b. In the following analysis we use $\mu = 4.8$ GeV. On the lattice we measure the "B parameters"

$$B_X^{lat}(1/a) \equiv \frac{\langle \bar{B}^0 | O_X^{lat}(1/a) | B^0 \rangle}{\frac{8}{3}\langle \bar{B}^0 | A_4^{lat}(1/a) | 0 \rangle \langle 0 | A_4^{lat}(1/a) | B^0 \rangle}, \quad (5.2)$$

for four-quark operators $O_X = O_L$, O_S, O_R, O_N, and O_M using the NRQCD action in Eq. (2.1). We performed the simulations on a quenched $16^3 \times 48$ lattice at $\beta = 5.9$. Other details of the lattice calculations are found in Ref. [14].

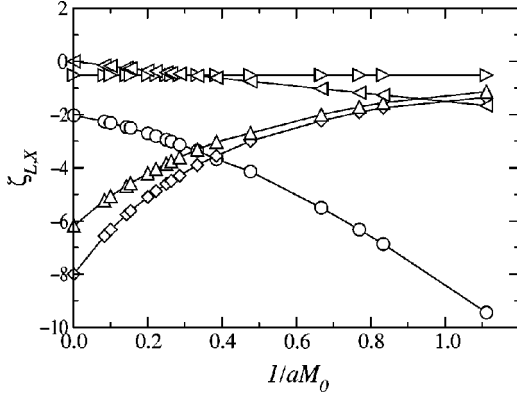The perturbative matching relation for the continuum operator O_L in Eq. (4.27) may be used to obtain

FIG. 6. $1/aM_0$ dependence of the one-loop coefficient for the matching of O_L. For ζ_L we plot $\zeta_{L,L} - 2\zeta_A$ (circle), and others are $\zeta_{L,S}$ (diamond), $\zeta_{L,R}$ (triangle right), $\zeta_{L,N}$ (triangle up), and $\zeta_{L,M}$ (triangle left).

$$B_L(\mu) = Z_{L,L/A^2}(\mu,a)B_L^{lat}(1/a) + Z_{L,S/A^2}B_S^{lat}(1/a)$$
$$+ Z_{L,R/A^2}B_R^{lat}(1/a) + Z_{L,N/A^2}B_N^{lat}(1/a)$$
$$+ Z_{L,M/A^2}B_M^{lat}(1/a), \qquad (5.3)$$

where the matching factors are

$$Z_{L,L/A^2}(\mu,a) = 1 + \frac{\alpha_s}{4\pi}\left(2\ln\frac{M_0^2}{\mu^2} + \zeta_{L,L} - 2\zeta_A\right), \quad (5.4)$$

$$Z_{L,S/A^2} = \frac{\alpha_s}{4\pi}\zeta_{L,S}, \qquad (5.5)$$

$$Z_{L,R/A^2} = \frac{\alpha_s}{4\pi}\zeta_{L,R}, \qquad (5.6)$$

$$Z_{L,N/A^2} = \frac{\alpha_s}{4\pi}\zeta_{L,N}, \qquad (5.7)$$

$$Z_{L,M/A^2} = \frac{\alpha_s}{4\pi}\zeta_{L,M}. \qquad (5.8)$$

The one-loop coefficients $\zeta_{L,X}$ are defined in Eq. (4.27) and plotted in Fig. 6 as a function of $1/aM_0$. The coefficient of the leading contribution $\zeta_{L,L} - 2\zeta_A$ becomes larger in magnitude toward lighter heavy quark. The mass dependence of $\zeta_{L,L} - 2\zeta_A$ is relatively smaller than that of $\zeta_{L,L}$ itself, due to the cancellation of singlet diagrams (Fig. 2) against the contribution of the denominator $-2\zeta_A$. Two mixing coefficients $\zeta_{L,S}$ and $\zeta_{L,N}$ become smaller when $1/M$ correction is incorporated. It is also important that $\zeta_{L,M}$, which vanishes in the static limit, becomes nonzero for finite heavy quark mass.

The matrix elements on the lattice $B_X^{lat}(1/a)$ measured in Ref. [14] are shown in Fig. 7 as a function of inverse meson mass $1/M_P$. Their mass dependence is qualitatively well described by the vacuum saturation approximation.
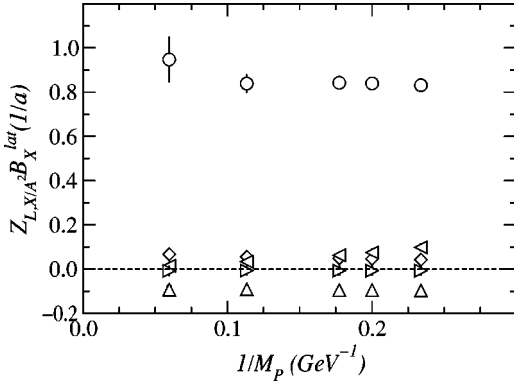

FIG. 7. Matrix elements $B_X^{lat}(1/a)$ in Eq. (5.2) measured on the lattice. Dashed curves represent a quadratic fit to the data, and the extrapolated static limit is shown by a open symbol.

FIG. 8. Contribution of individual operators $Z_{L,X/A^2} B_X^{lat}(1/a)$ to $B_L(\mu)$. Symbols are $X = L$ (circle), S (diamond), R (triangle right), N (triangle up), and M (triangle left).

For the coupling constant α_s we choose the *V*-scheme coupling $\alpha_V(q^*)$ [12] with $q^* = 2/a$. To estimate the size of higher order perturbative errors we also analyze with $q^* = 1/a$ and π/a.

Combining $Z_{L,X/A^2}$ and B_X^{lat} we obtain the contribution of each term $Z_{L,X/A^2} B_X^{lat}(1/a)$ in Eq. (5.3) as shown in Fig. 8. In spite of the large mass dependence of the coefficients $\zeta_{L,S}$ and $\zeta_{L,N}$, there is no significant mass dependence in the corresponding combined quantities $Z_{L,X/A^2} B_X^{lat}(1/a)$, since those are canceled by the large and opposite mass dependence in $B_S^{lat}(1/a)$ and $B_N^{lat}(1/a)$. A small increase of $Z_{L,M/A^2} B_M^{lat}(1/a)$ from zero in the static limit is observed, which reflects the increasing trend of both $Z_{L,M/A^2}$ and $B_M^{lat}(1/a)$.

The total result for $B_L(m_b)$ is presented in Fig. 9 by filled circles. Because of the cancellation of the large mass dependences in $\zeta_{L,X}$ and in $B_X^{lat}(1/a)$, there is little $1/M_P$ dependence in our final result (filled circles). A small increase toward larger $1/M_P$ comes from the contribution of O_M. In
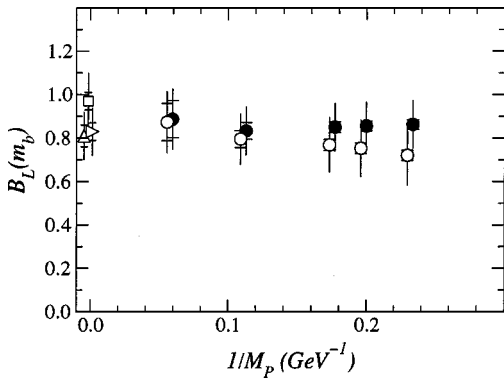

FIG. 9. $1/M_P$ dependence of $B_L(m_b)$ obtained with the NRQCD action (filled circles). The same calculation but with the matching coefficient in the infinite mass limit is shown by open circles. Other symbols in the static limit are calculations with the static action by UKQCD [2] (triangle up), Giménez and Martinelli [3] (triangle right) and Christensen *et al.* [4] (square). We reanalyzed their raw data with the same method as ours, namely we used Eqs. (5.3)–(5.8) with $\alpha_V(2/a)$ and ζ's in the static limit.

this plot our estimate of systematic uncertainty is shown by error bars. The horizontal ticks attached to the error bars represent the size of the statistical error, which is much smaller than the systematic errors especially for large $1/M_P$ points.

We also plot our previous analysis with the same NRQCD action but using the perturbative matching in the static limit (open circles in Fig. 9). There is a small negative slope in $1/M_P$ so that the previous result is about 12% smaller than our new result at the *B* meson mass. An estimation of $\mathcal{O}(\alpha_s/(aM_b))$ error in our previous analysis is around 10%, when we assume an order counting argument with typical value of the strong coupling constant $\alpha_s \sim 0.3$. In addition to this error, there are also other errors of $\mathcal{O}(\alpha_s^2)$, $\mathcal{O}(a^2\Lambda_{QCD}^2)$, and $\mathcal{O}(\alpha_s a\Lambda_{QCD})$. Thus the shift of our result does not exceed the systematic uncertainty discussed in Ref. [14].

Our final numerical result is

$$B_L(m_b) = 0.85 \pm 0.03 \pm 0.11, \qquad (5.9)$$

where the first error is statistical and the second is systematic. The systematic error is estimated using the order counting of neglected contributions. In our new analysis in which the $\mathcal{O}(\alpha_s/(aM_b))$ error is removed, the remaining sources of uncertainty are the dicretization errors $\mathcal{O}(a^2\Lambda_{QCD}^2)$ ($\sim 5\%$) and $\mathcal{O}(\alpha_s a\Lambda_{QCD})$ ($\sim 5\%$), as well as higher order perturbative error $\mathcal{O}(\alpha_s^2)$ ($\sim 10\%$). Higher order contributions in the nonrelativistic expansion are $\mathcal{O}(\alpha_s\Lambda_{QCD}/M_b)$ ($\sim 2\%$) and $\mathcal{O}(\Lambda_{QCD}^2/M_b^2)$ ($< 1\%$), which are not dominant uncertainties. We assume $\alpha_s \sim 0.3$ and $\Lambda_{QCD} \sim 350$ MeV when we estimate the errors listed above, which are added in quadrature to give the systematic error of about 13% in the final result.

The result (5.9) may be compared with the recent lattice calculations with relativistic heavy quark actions: $0.92(4)^{+3}_{-0}$ [22] and $0.93(8)^{+0.0}_{-0.6}$ [23], where the first error is statistical and the second is their estimate of systematic errors. It is encouraging that our result agrees with these relativistic calculations within the large systematic uncertainty in Eq. (5.9). Although the systematic error in the relativistic results seems much smaller, it should be noted that the quoted systematic uncertainty could be underestimated. They extrapolate their simulation results performed around the charm mass regime assuming the $1/M$ scaling without considering $O((aM_0)^2)$ errors. However, the $1/M$ dependence of the simulation results could be distorted by the $\mathcal{O}((aM_0)^2)$ error, which can be as large as 30% toward the heavier side in the naive order counting. In order to have a reliable prediction of $B_L(m_b)$, one has to at least include $O((aM_0)^2)$ error when extrapolating in $1/M$, or take a careful contiuum limit before doing $1/M$ extrapolation. Furthermore, the heavy quark expansion becomes questionable to describe the heavy quark in the charm quark mass regime when truncated at $1/M$ or at $1/M^2$. Therefore, an alternative method to fit the results would be to include the result in the static limit in order to constrain at least the leading term in the $/1M$ expansion.

Finally, we also obtain chiral breaking effect on the ratio of B_L as

$$\frac{B_{B_s}(m_{B_s})}{B_{B_d}(m_{B_d})} = 1.01 \pm 0.01 \pm 0.03, \tag{5.10}$$

for which the relativistic results are 0.98(3) [22] and 0.98(5) [23].

B. B_S

The B parameter B_S is defined as

$$B_S(\mu) \equiv \frac{\langle \bar{B}^0 | O_S^{\overline{\mathrm{MS}}}(\mu) | B^0 \rangle}{\frac{5}{3} \langle \bar{B}^0 | P^{\overline{\mathrm{MS}}}(\mu) | 0 \rangle \langle 0 | P^{\overline{\mathrm{MS}}}(\mu) | B^0 \rangle}. \tag{5.11}$$

We also define a ratio of the matrix elements of bilinear operators

$$\mathcal{R}(\mu) \equiv \left| \frac{\langle 0 | A_4^{\overline{\mathrm{MS}}} | B^0 \rangle}{\langle 0 | P^{\overline{\mathrm{MS}}}(\mu) | B^0 \rangle} \right|, \tag{5.12}$$

and calculate

$$\frac{B_S(\mu)}{\mathcal{R}(\mu)^2} = \frac{\langle \bar{B}^0 | O_S^{\overline{\mathrm{MS}}}(\mu) | B^0 \rangle}{-\frac{5}{3} \langle \bar{B}^0 | A_4^{\overline{\mathrm{MS}}} | 0 \rangle \langle 0 | A_4^{\overline{\mathrm{MS}}} | B^0 \rangle}, \tag{5.13}$$

which is necessary in evaluating the B_s meson width difference [24].

In the lattice simulation we measure

$$B_X'^{lat}(1/a) \equiv \frac{\langle \bar{B}^0 | O_X^{lat}(1/a) | B^0 \rangle}{-\frac{5}{3} \langle \bar{B}^0 | A_4^{lat}(1/a) | 0 \rangle \langle 0 | A_4^{lat}(1/a) | B^0 \rangle}, \tag{5.14}$$

for four-quark operators $O_X = O_S$, O_L, O_R, O_P, and O_T. Note that the denominator of $B_X'^{lat}$ is different from Eq. (5.11). The perturbative matching relation for the continuum operator $O_S^{\overline{\mathrm{MS}}}$ in Eq. (4.38) may be used to obtain

$$\frac{B_S(\mu)}{\mathcal{R}(\mu)^2} = Z_{S,S/A^2}(\mu,a) B_S'^{lat}(1/a) + Z_{S,L/A^2}(\mu,a) B_L'^{lat}(1/a)$$

$$+ Z_{S,R/A^2} B_R'^{lat}(1/a) + Z_{S,P/A^2} B_P'^{lat}(1/a)$$

$$+ Z_{S,T/A^2} B_T'^{lat}(1/a), \tag{5.15}$$

where

$$Z_{S,S/A^2}(\mu,a) = 1 + \frac{\alpha_s}{4\pi} \left(\frac{16}{3} \ln \frac{\mu^2}{M_0^2} - \frac{8}{3} \ln(a^2 M_0^2) \right.$$
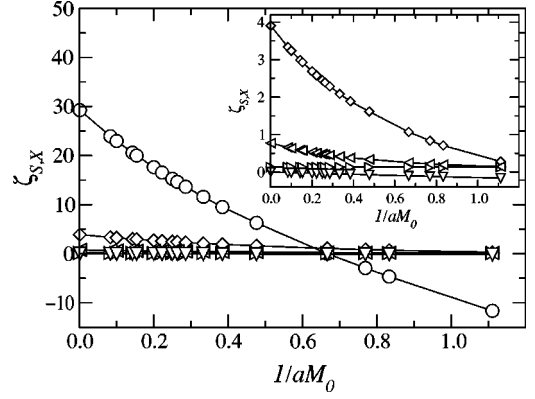
$$\left. + \zeta_{S,S} - 2\zeta_A \right), \tag{5.16}$$

FIG. 10. $1/aM_0$ dependence of the one-loop coefficient for the matching of O_S. For ζ_S we plot $\zeta_{S,S} - 2\zeta_A$ (circle), and others are $\zeta_{S,L}$ (diamond), $\zeta_{S,R}$ (triangle right), $\zeta_{S,P}$ (triangle left), and $\zeta_{S,T}$ (triangle down).

$$Z_{S,L/A^2}(\mu,a) = \frac{\alpha_s}{4\pi} \left(\frac{1}{3} \ln \frac{\mu^2}{M_0^2} - \frac{2}{3} \ln(a^2 M_0^2) + \zeta_{S,L} \right), \tag{5.17}$$

$$Z_{S,R/A^2} = \frac{\alpha_s}{4\pi} \zeta_{S,R}, \tag{5.18}$$

$$Z_{S,P/A^2} = \frac{\alpha_s}{4\pi} \zeta_{S,P}, \tag{5.19}$$

$$Z_{S,T/A^2} = \frac{\alpha_s}{4\pi} \zeta_{S,T}. \tag{5.20}$$

The one-loop coefficients $\zeta_{S,X}$ defined in Eq. (4.38) are plotted in Fig. 10 as a function of $1/aM_0$. The $1/M_0$ dependence is quite large for the leading contribution $\zeta_{S,S} - 2\zeta_A$, because the denominator in Eq. (5.13) is not a vacuum saturation of the numerator and the cancellation of color singlet diagrams (Fig. 2) does not take place. Among other coefficients, $\zeta_{S,L}$ has relatively large $1/M_0$ dependence and the mixing of operator O_L becomes smaller as $1/aM_0$ increases.

The matrix elements $B_X^{lat}(1/a)$ are shown in Fig. 11. The $1/M_P$ dependence in B_S, B_P, and B_T is significant, which is well described by the vacuum saturation approximation as discussed in Ref. [24]. The contribution of each term $Z_{S,X/A^2} B_X^{lat}(1/a)$ in Eq. (5.15) to $B_S(m_b)/\mathcal{R}(m_b)^2$ is plotted in Fig. 12, in which no clear $1/M_P$ dependence is observed.

The total result for $B_S(m_b)/\mathcal{R}(m_b)^2$ is presented in Fig. 13 by filled circles. As is evident from the plot of each term $Z_{S,X/A^2} B_X^{lat}(1/a)$ (Fig. 12), there is no clear trend in the $1/M_P$ dependence of $B_S(m_b)/\mathcal{R}(m_b)^2$. Our previous analysis [24] with matching coefficients in the static limit is plotted with open symbols. Reduction of the result with the correction is quite large ($\sim 20\%$), but consistent with our estimate for the collection of systematic errors of $\mathcal{O}(\alpha_s/(aM))$, $\mathcal{O}(\alpha_s^2)$, and $\mathcal{O}(a^2 \Lambda_{QCD}^2)$, $\mathcal{O}(\alpha a \Lambda_{QCD})$ ($\sim 20\%$). The main effect comes from the large $1/aM_0$ dependence of $\zeta_{S,S} - 2\zeta_A$ shown in Fig. 10.
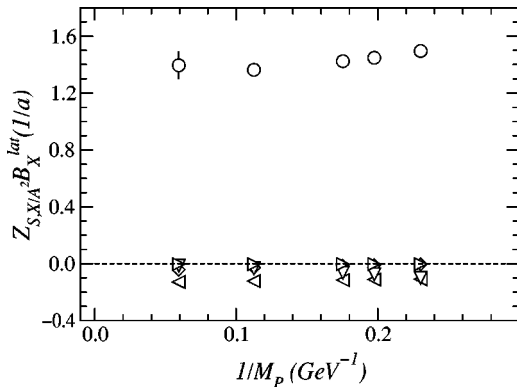
Our final numerical result is
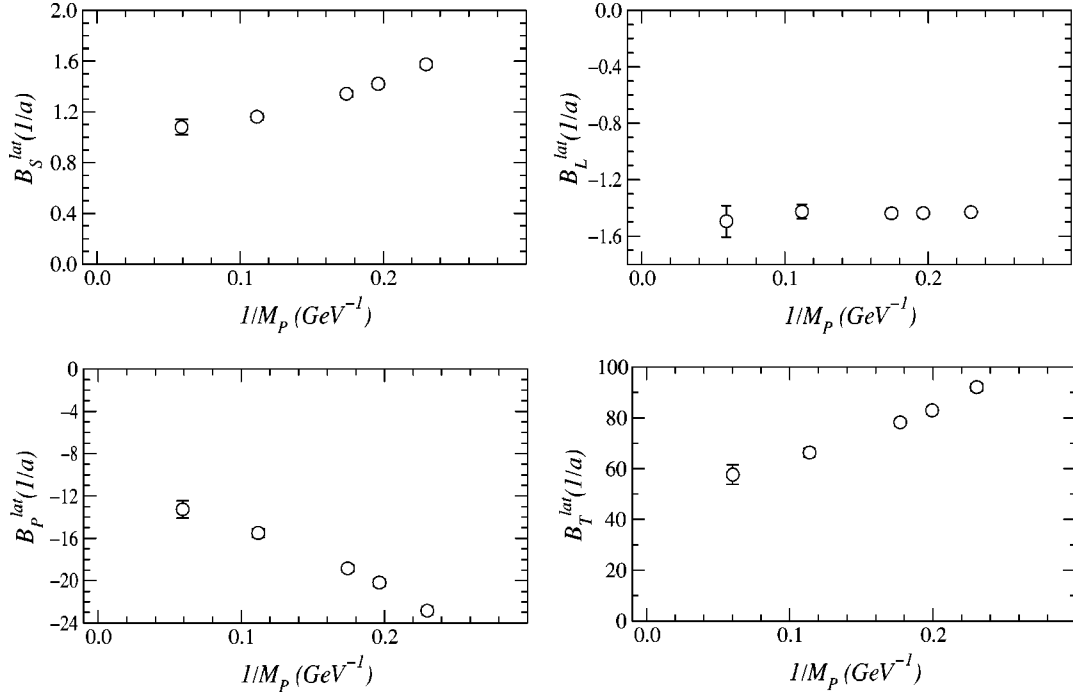
FIG. 11. Matrix elements $B_X^{lat}(1/a)$ in Eq. (5.14) measured on the lattice.

$$\frac{B_S(m_b)}{\mathcal{R}(m_b)^2} = 1.24 \pm 0.03 \pm 0.16, \qquad (5.21)$$

where the first error is a statistical one, and the second is our estimate of systematic uncertainty obtained as in the analysis of B_L. For the width difference we obtain

$$\left(\frac{\Delta\Gamma}{\Gamma}\right)_{B_s} = 0.107 \pm 0.026 \pm 0.014 \pm 0.017 \qquad (5.22)$$
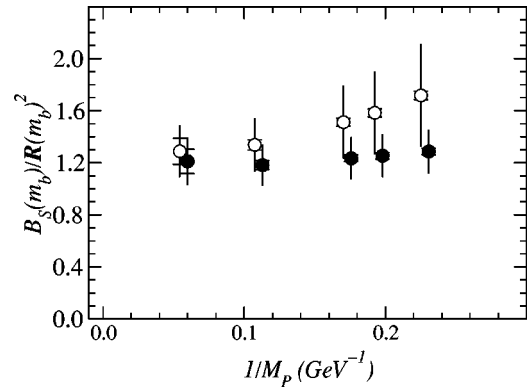
using Eq. (9) of Ref. [24]. Errors are from the B_s meson decay constant $f_{B_s} = 245(30)$ MeV, which is taken from the current world average of unquenched lattice calculations [1], from $B_S(m_b)/\mathcal{R}(m_b)^2$, and from an estimate of the higher order contribution in the $1/m_b$ expansion [29,30].

VI. CONCLUSIONS

In this paper we have performed one-loop calculations of matching coefficients for $\Delta B = 2$ four-quark operators defined using lattice NRQCD. This calculation allows us to remove one of the dominant systematic errors characterized by $\mathcal{O}(\alpha_s/(aM_b))$ from the lattice simulation of the B parameters B_L and B_S. We find sizable $1/aM_0$ dependence in several one-loop coefficients, which affects the mass dependence of the B parameters as well as their absolute values at the b quark mass.

We have also presented a reanalysis of our previous simulations and obtained results for B_L and for $B_S/\mathcal{R}^2$ with reduced systematic error. The difference from our previous results is consistent with the estimate obtained with order counting argument. Remaining systematic uncertainty is

FIG. 12. Contribution of individual operators $Z_{S,X/A^2}B_X^{lat}(1/a)$ to $B_S(\mu)/\mathcal{R}(\mu)^2$. Symbols are $X = S$ (circle), L (diamond), R (triangle right), P (triangle left), and T (triangle down).

FIG. 13. $1/M_P$ dependence of $B_S(m_b)/\mathcal{R}(m_b)^2$ obtained with the NRQCD action (filled circles). The same calculation but with the matching coefficient in the infinite mass limit is shown by open circles.

dominated by unknown two-loop matching coefficients.

APPENDIX A: LATTICE NRQCD FEYNMAN RULES

In order to simply the expression, we set the lattice spacing $a = 1$ throughout Appendices A and B. When deriving the Feynman rules from the NRQCD action, we followed the method which is explained in Ref. [26]. We also note that the Feynman rules for $O(1/M)$ NRQCD action with slightly different definition from ours are given in Ref. [28].

1. Functions

We define the following functions which appear in the Feynman rules below:

$$\tilde{l}^2 \equiv \sum_{\mu=1}^{4} 4 \sin^2 \frac{l_\mu}{2}, \tag{A1}$$

$$A^{(0)}(l) \equiv 1 - \frac{1}{nM_0} \sum_{i=1}^{3} \sin^2 \frac{l_i}{2}, \tag{A2}$$

$$C(l',l) \equiv e^{-il'_4} + e^{-il_4}, \tag{A3}$$

$$f^A_{\mu\nu}(q) \equiv \sin q_\mu \cos \frac{q_\nu}{2}, \tag{A4}$$

$$f^B_{\mu\nu}(q_1,q_2) \equiv \cos\left(\frac{q_1+q_2}{2}\right)_\mu \sin\left(\frac{q_1+q_2}{2}\right)_\nu \sin\left(\frac{q_1-q_2}{2}\right)_\mu, \tag{A5}$$

$$f^C_{\mu\nu}(q_1,q_2) \equiv \frac{1}{2}\left[\cos\left(\frac{q_1}{2}\right)_\mu \cos\left(q_1+\frac{q_2}{2}\right)_\nu + \cos\left(q_2+\frac{q_1}{2}\right)_\mu \cos\left(\frac{q_2}{2}\right)_\nu \right.$$
$$\left. + \cos\left(q_2+\frac{q_1}{2}\right)_\mu \cos\left(q_1+\frac{q_2}{2}\right)_\nu - \cos\left(\frac{q_1}{2}\right)_\mu \cos\left(\frac{q_2}{2}\right)_\nu \right]. \tag{A6}$$

We also define

$$A^{(1)}(l',l;p_1,\mu_1) \equiv \frac{-1}{2nM_0}\left[\sum_{i=0}^{n-1} A^{(0)}(l')^i A^{(0)}(l)^{n-1-i}\right] \sin\left(\frac{l'+l}{2}\right)_{\mu_1}, \tag{A7}$$

$$A_1^{(2)}(l',l;p_1,\mu_1,p_2,\mu_2) \equiv \frac{-1}{4nM_0}\left[\sum_{i=0}^{n-1} A^{(0)}(l')^i A^{(0)}(l)^{n-1-i}\right] \cos\left(\frac{l'+l}{2}\right)_{\mu_1}, \tag{A8}$$

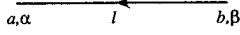$$A_2^{(2)}(l',l,p_1,\mu_1,p_2,\mu_2) \equiv \frac{1}{(2nM_0)^2}\left[\sum_{i=0}^{n-2}\sum_{j=0}^{n-2-i} A^{(0)}(l')^j A^{(0)}(l-p_2)^i A^{(0)}(l)^{n-2-i-j}\right]$$
$$\times \sin\left(l'+\frac{p_1}{2}\right)_{\mu_1} \sin\left(l-\frac{p_2}{2}\right)_{\mu_2}, \tag{A9}$$

$$dH_1^{(1)}(l',l;p_1,\mu_1) \equiv +i\frac{c_B}{4M_0}\sum_{i,j=1}^{3} \epsilon_{ij\mu_1} \Sigma^i f^A_{j\mu_1}(p_1), \tag{A10}$$

$$dH_2^{(2)}(l',l;p_1,\mu_1,p_2,\mu_2) \equiv -i\frac{c_B}{4M_0}\sum_{i,j=1}^{3}\epsilon_{ij\mu_1}\Sigma^i f_{j\mu_1}^B(p_1,p_2), \tag{A11}$$

$$dH_3^{(2)}(l',l;p_1,\mu_1,p_2,\mu_2) \equiv -i\frac{c_B}{4M_0}\sum_{i=1}^{3}\epsilon_{i\mu_1\mu_2}\Sigma^i f_{\mu_1\mu_2}^C(p_1,p_2), \tag{A12}$$

where Σ^i denotes a four-by-four matrix

$$\Sigma^i = \begin{pmatrix} \sigma^i & 0 \\ 0 & \sigma^i \end{pmatrix}. \tag{A13}$$

Using these functions the Fourier components of the evolution operator in Eq. (2.2) is written as

$$v_K^{(1)}(l',l;p_1,\mu_1) = [(e^{-il_4'}A^{(0)}(l')^n + e^{-il_4}A^{(0)}(l)^n)A^{(1)}(l',l;p_1,\mu_1)$$
$$+A^{(0)}(l')^nA^{(0)}(l)^nC(l',l)dH_1^{(1)}(l',l;p_1,\mu_1)]\hat{\delta}_{4\mu_1} - ie^{-(1/2)(l_4'+l_4)}A^{(0)}(l')^nA^{(0)}(l)^n\delta_{4\mu_1}, \tag{A14}$$

$$v_K^{(2)}(l',l;p_1,\mu_1,p_2,\mu_2) = -\frac{1}{2}e^{-(i/2)(l_4'+l_4)}\delta_{4\mu_1}\delta_{\mu_1\mu_2} + [(e^{-il_4'}A^{(0)}(l')^n + e^{-il_4}A^{(0)}(l)^n)A_2^{(2)}(l',l;p_1,\mu_1,p_2,\mu_2)$$
$$+e^{-i(l-p_2)_4}A^{(1)}(l',l-p_2;p_1,\mu_1)A^{(1)}(l-p_2,l;p_2,\mu_2)$$
$$+A^{(0)}(l')^nC(l',l-p_2)A^{(1)}(l-p_2,l;p_2,\mu_2)dH_1^{(1)}(l',l-p_2;p_1,\mu_1)$$
$$+A^{(0)}(l)^nC(l-p_2,l)A^{(1)}(l',l-p_2;p_1,\mu_1)dH_1^{(1)}(l-p_2,l;p_2,\mu_2)$$
$$+A^{(0)}(l')^nA^{(0)}(l)^nC(l',l)dH_3^{(2)}(l',l;p_1,\mu_1,p_2,\mu_2)$$
$$+e^{-i(l-p_2)_4}A^{(0)}(l')^nA^{(0)}(l)^ndH_1^{(1)}(l',l-p_2;p_1,\mu_1)dH_1^{(1)}(l-p_2,l;p_2,\mu_2)]\hat{\delta}_{4\mu_1}\hat{\delta}_{4\mu_2}$$
$$+[(e^{-il_4'}A^{(0)}(l')^n + e^{-il_4}A^{(0)}(l)^n)A_1^{(2)}(l',l;p_1,\mu_1,p_2,\mu_2)$$
$$+A^{(0)}(l')^nA^{(0)}(l)^nC(l',l)dH_2^{(2)}(l',l;p_1,\mu_1,p_2,\mu_2)]\hat{\delta}_{4\mu_1}\delta_{\mu_1\mu_2}, \tag{A15}$$

where $\hat{\delta}_{4\mu} \equiv 1 - \delta_{4\mu}$.

2. Feynman rules

We summarize the Feynman rules used in our calculation.

In our convention the arrows in the heavy (anti-)quark propagator represent the flow of momentum irrespective of whether it is particle Q or anti-particle χ. Other notations are

a, b, ... color index of quarks,
α, β, ... spin index of quarks,
l, l' momentum of quarks,
A, B, ... color index of gluons,
μ, ν, ... spin index of gluons,
k, k_1, ... momentum of gluons.

Double lines denote the heavy (anti-)quark propagators.

We also need Feynman rules for heavy-light bilinear and four-quark operators. In this appendix, we give the Feynman rules for $\Delta B = -1$ heavy-light current as an illustration. Feynman rules for other operators can easily be deduced.

In the diagrams involving a heavy-light current, heavy quark is incoming into the current, and heavy anti-quark is outgoing from the current. Light quark represented by a single line is, on the other hand, always outgoing.

Gluon propagator:

$$\delta^{AB}\delta_{\mu\nu}G(k) \equiv \delta^{AB}\delta_{\mu\nu}\frac{1}{\tilde{k}^2 + \lambda^2}. \tag{A16}$$
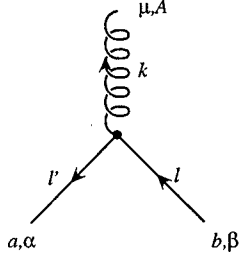
Light quark propagator:

$$\delta_{ab}\left[-i\sum_{\mu=1}^{4}\gamma_\mu\sin l_\mu+\frac{r}{2}\tilde{l}^2\right]_{\alpha\beta}S(l),$$

$$\text{where}\quad S(l)^{-1}=\sum_{\mu=1}^{4}\sin^2 l_\mu+\left(\frac{r}{2}\tilde{l}^2\right)^2 . \tag{A17}$$
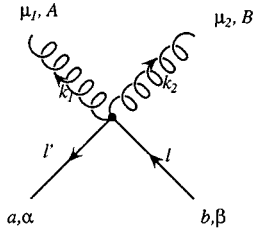
$\mathcal{O}(g)$ vertex for light quark:

$$g(T^A)_{ab}\left[-i\gamma_\mu\cos\left(\frac{l'+l}{2}\right)_\mu-r\sin\left(\frac{l'+l}{2}\right)_\mu\right.$$
$$\left.+\frac{i}{2}rc_{sw}\sum_{\lambda=1}^{4}f^A_{\lambda\mu}(k)\sigma_{\lambda\mu}\right]_{\alpha\beta} . \tag{A18}$$

$\mathcal{O}(g^2)$ vertex for light quark:
The vertex from the clover term does not give any contribution to the diagrams we compute, thus we do not give the explcit expression here.

$$-\frac{g^2}{2}\{T^A,T^B\}_{ab}\left[r\cos\left(\frac{l'+l}{2}\right)_{\mu_1}\right.$$
$$\left.-i\gamma_{\mu_1}\sin\left(\frac{l'+l}{2}\right)_{\mu_1}\right]_{\alpha\beta}\delta_{\mu_1\mu_2}$$

$$+\text{contribution from the clover term} \quad . \tag{A19}$$

Heavy quark propagator:
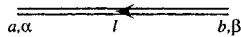
$$\delta_{ab}\left(\frac{1+\gamma_4}{2}\right)_{\alpha\beta}Q(l)$$
$$\equiv\left(\frac{1+\gamma_4}{2}\right)_{\alpha\beta}\frac{\delta_{ab}}{1-e^{-il_4}A^{(0)}(l)^{2n}} \quad . \tag{A20}$$

$\mathcal{O}(g^2)$ counter term introduced for the tadpole improvement:
This term appears because we divide all the link variables U_μ in the NRQCD action by the mean field value of $u_0=1-g^2u^{(2)}$.
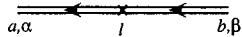
$$\frac{g^2u_0^{(2)}}{M_0}\delta_{ab}\left(\frac{1+\gamma_4}{2}\right)_{\alpha\beta}$$

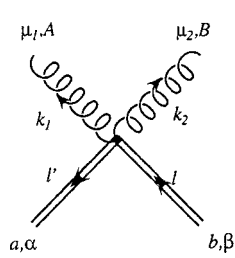$$\times e^{-il_4}A^{(0)}(l)^{2n-1}\left[2\kappa_2(l)-3-M_0A^{(0)}(l)\right] . \tag{A21}$$

$\mathcal{O}(g)$ vertex for heavy quark:
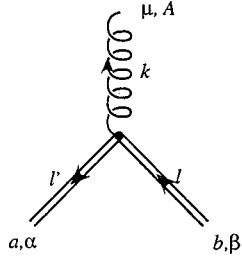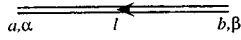

$$g(T^A)_{ab}\left[v_K^{(1)}(l',l;k,\mu)\frac{1+\gamma_4}{2}\right]_{\alpha\beta}\ . \tag{A22}$$

$\mathcal{O}(g^2)$ vertex for vertex:

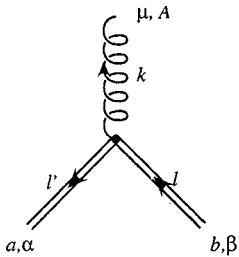$$g^2\left(\left[(T^AT^B)_{ab}v_K^{(2)}(l',l;k_1,\mu_1,k_2,\mu_2)\right.\right.$$
$$\left.\left.+(T^BT^A)_{ab}v_K^{(2)}(l',l;k_2,\mu_2,k_1,\mu_1)\right]\frac{1+\gamma_4}{2}\right)_{\alpha\beta}\ . \tag{A23}$$

Heavy anti-quark propagator:

$$\delta_{ab}\left(\frac{1-\gamma_4}{2}\right)_{\alpha\beta}Q(l)$$
$$\equiv\left(\frac{1-\gamma_4}{2}\right)_{\alpha\beta}\frac{\delta_{ab}}{1-e^{-il_4}A^{(0)}(l)^{2n}}\ . \tag{A24}$$

$\mathcal{O}(g)$ vertex for heavy anti-quark:

$$-g\left[\Sigma^2 v_K^{(1)}(l',l;p,\mu)\Sigma^2\frac{1-\gamma_4}{2}\right]_{\beta\alpha}(T^A)_{ba}\ . \tag{A25}$$

Heavy-light current:
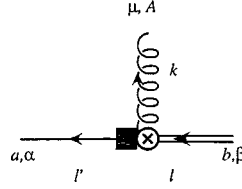

$$\left[\Gamma\frac{1+\gamma_4}{2}\right]_{\alpha\beta}\delta_{ab}\ . \tag{A26}$$

Heavy-light current with the FWT rotation:

$$\left[\Gamma\frac{-i}{2M_0}\sum_{i=1}^{3}\gamma_i\sin l_i\frac{1+\gamma_4}{2}\right]_{\alpha\beta}\delta_{ab}\ . \tag{A27}$$
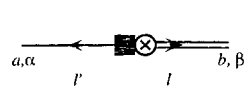
Vertex from rotated heavy-light current:

$$\left[\Gamma \frac{-ig}{2M_0} \gamma_\mu \cos\left(l - \frac{k}{2} \right)_\mu \frac{1 + \gamma_4}{2} \right]_{\alpha\beta} (T^A)_{ab} \hat{\delta}_{\mu_4} . \tag{A28}$$
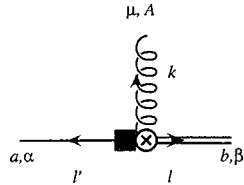
(Anti-)heavy-light current:

$$\left[\Gamma \frac{1 - \gamma_4}{2} \right]_{\alpha\beta} \delta_{ab} . \tag{A29}$$

(Anti-)heavy-light current with the FWT rotation:

$$\left[\Gamma \frac{i}{2M_0} \sum_{i=1}^{3} \gamma_i \sin l_i \frac{1 - \gamma_4}{2} \right]_{\alpha\beta} \delta_{ab} . \tag{A30}$$

Vertex from rotated (anti-)heavy-light current:

$$\left[\Gamma \frac{-ig}{2M_0} \gamma_\mu \cos\left(l + \frac{k}{2} \right)_\mu \frac{1 - \gamma_4}{2} \right]_{\alpha\beta} (T^A)_{ab} \hat{\delta}_{\mu_4} . \tag{A31}$$

APPENDIX B: ONE-LOOP INTEGRALS

We list the integrals appearing in the one-loop calculations with the NRQCD action:

$$I_A = \int \frac{d^4 l}{(2\pi)^4} G(l) S(-l) Q(-l) \left[\left(\cos\frac{l_4}{2} \sin l_4 + \frac{1}{2} \tilde{l}^2 \sin\frac{l_4}{2} \right) Z(l) + \sum_{i=1}^{3} \left(\sin^2 l_i + \tilde{l}^2 \sin^2 \frac{l_i}{2} \right) \frac{1}{2} X(l) + \frac{i}{2} \left(1 + \frac{c_{sw}}{4} \tilde{l}^2 \right) \right.$$
$$\left. \times \left(\sum_{i=1}^{3} \sin^2 l_i \sum_{j=1}^{3} \cos^2 \frac{l_j}{2} - \sum_{i=1}^{3} \sin^2 l_i \cos^2 \frac{l_i}{2} \right) Y(l) \right] - \int \frac{d^4 l}{(2\pi)^4} \frac{\theta(1 - l^2)}{(l^2)^2} , \tag{B1}$$

$$I_B = \int \frac{d^4 l}{(2\pi)^4} G(l) S(-l) Q(-l) \left[-i \left(-\sin\frac{l_4}{2} \sin l_4 + \frac{1}{2} \tilde{l}^2 \cos\frac{l_4}{2} - \frac{c_{sw}}{2} \cos\frac{l_4}{2} \sum_{i=1}^{3} \sin^2 l_i \right) Z(l) \right.$$
$$\left. + i \sum_{i=1}^{3} \left(\sin^2 \frac{l_i}{2} - \frac{c_{sw}}{4} \sin^2 l_i \right) \sin l_4 X(l) \right] , \tag{B2}$$

$$I_C = \int \frac{d^4 l}{(2\pi)^4} G(l) S(-l) Q(-l) \left[-\frac{i}{6} \left(1 + \frac{c_{sw}}{4} \tilde{l}^2 \right) \left(\sum_{i=1}^{3} \sin^2 l_i \sum_{j=1}^{3} \cos^2 \frac{l_j}{2} - \sum_{i=1}^{3} \sin^2 l_i \cos^2 \frac{l_i}{2} \right) Y(l) \right] , \tag{B3}$$

$$I_D = \int \frac{d^4l}{(2\pi)^4} G(l) S(-l) Q(-l) \frac{1}{6M_0} \left[\sum_{i=1}^{3} \sin^2 l_i \left(-\sin\frac{l_4}{2} + \frac{c_{sw}}{2}\cos\frac{l_4}{2}\sin l_4 \right) Z(l) \right.$$

$$+ \sum_{i=1}^{3} \sin^2 l_i \left(\sin^2\frac{l_4}{2} - \frac{c_{sw}}{4}\sin^2 l_4 \right) X(l) - \frac{i}{2}\left(\tilde{l}^2 - c_{sw}\sum_{\mu=1}^{4}\sin^2 l_\mu \right)\left(\sum_{i=1}^{3}\cos^2\frac{l_i}{2}\sum_{j=1}^{3}\sin^2 l_j \right.$$

$$\left. \left. - \sum_{i=1}^{3}\sin^2 l_i \cos^2\frac{l_i}{2} \right) Y(l) \right], \tag{B4}$$

$$I_E = \int \frac{d^4l}{(2\pi)^4} G(l) S(-l) Q(-l) \frac{i}{6M_0}\left(1 + \frac{c_{sw}}{4}\tilde{l}^2 \right)\left[\left(\cos\frac{l_4}{2}Z(l) - \frac{1}{2}\sin l_4 X(l) \right)\sum_{i=1}^{3}\sin^2 l_i \right.$$

$$\left. + i\left(\sum_{i=1}^{3}\sin^2 l_i \sum_{j=1}^{3}\cos^2\frac{l_j}{2} - \sum_{i=1}^{3}\sin^2 l_i \cos^2\frac{l_i}{2} \right)\sin l_4 Y(l) \right], \tag{B5}$$

$$I_F = -\int \frac{d^4l}{(2\pi)^4} G(l) S(-l) \frac{1}{12M_0}\sum_{i=1}^{3}\left(\tilde{l}^2\cos^2\frac{l_i}{2} - \sin^2 l_i + c_{sw}\sin^2 l_i \cos^2\frac{l_i}{2} - c_{sw}\sum_{\mu=1}^{4}\sin^2 l_\mu \cos^2\frac{l_i}{2} \right), \tag{B6}$$

$$I_G = -\int \frac{d^4l}{(2\pi)^4} G(l) Q(-l)^2\left(\sum_{i=1}^{3}\sin^2\frac{l_i}{2}X(l)^2 + Z(l)^2 \right) + \int \frac{d^4l}{(2\pi)^4}\left[\frac{2M_0}{-2iM_0 l_4 + l^2} \right]^2\frac{\theta(1-l^2)}{l^2} - \frac{4}{(4\pi)^2}\sinh^{-1}\frac{1}{2M_0}, \tag{B7}$$

$$I_H = -\int \frac{d^4l}{(2\pi)^4} G(l) Q(-l)^2\frac{1}{3}\left(\sum_{i=1}^{3}\sin^2 l_i \sum_{j=1}^{3}\cos^2\frac{l_j}{2} - \sum_{i=1}^{3}\sin^2 l_i \cos^2\frac{l_i}{2} \right) Y(l)^2, \tag{B8}$$

$$I_I = -\int \frac{d^4l}{(2\pi)^4} G(l) Q(-l)^2\frac{1}{4M_0^2}\left[\frac{1}{3}Z(l)^2\sum_{i=1}^{3}\sin^2 l_i + \frac{1}{3}X(l)^2\sum_{i=1}^{3}\sin^2\frac{l_i}{2}\sum_{j=1}^{3}\sin^2 l_j \right.$$

$$\left. - \frac{1}{3}Y(l)^2\left(\sum_{i=1}^{3}\sin^2 l_i \sum_{j=1}^{3}\sin^2 l_j \sum_{k=1}^{3}\cos^2\frac{l_k}{2} - \sum_{i=1}^{3}\sin^2 l_i \cos^2\frac{l_i}{2}\sum_{j=1}^{3}\sin^2 l_j \right) \right], \tag{B9}$$

$$I_J = -\int \frac{d^4l}{(2\pi)^4} G(l)\frac{1}{12M_0^2}\sum_{i=1}^{3}\cos^2\frac{l_i}{2}, \tag{B10}$$

$$I_K = \int \frac{d^4l}{(2\pi)^4} G(l) Q(-l)\frac{1}{4M_0^2}\left[\frac{1}{6}\sum_{i=1}^{3}\sin^2 l_i X(l) - \frac{i}{3}\left(\sum_{i=1}^{3}\sin^2 l_i \sum_{j=1}^{3}\cos^2\frac{l_j}{2} - \sum_{i=1}^{3}\sin^2 l_i \cos^2\frac{l_i}{2} \right) Y(l) \right], \tag{B11}$$

$$I_L = -\int \frac{d^4l}{(2\pi)^4} G(l) S(-l)^2\frac{1}{12}\left(\sum_{\alpha,\beta=1}^{4}\sin^2 l_\alpha \cos^2\frac{l_\beta}{2} - \sum_{\alpha=1}^{4}\sin^2 l_\alpha \cos^2\frac{l_\alpha}{2} \right)\left(1 + \frac{1}{16}c_{sw}^2(\tilde{l}^2)^2 + \frac{1}{2}c_{sw}\tilde{l}^2 \right)$$

$$+ \int \frac{d^4l}{(2\pi)^4}\frac{\theta(1-l^2)}{4(l^2)^2}, \tag{B12}$$

$$I_M = \int \frac{d^4l}{(2\pi)^4} G(l) S(-l)^2\frac{1}{4}\left[-\sum_{\mu=1}^{4}\sin^2 l_\mu \sum_{\nu=1}^{4}\sin^2\frac{l_\nu}{2} - \frac{1}{4}c_{sw}^2\sum_{\mu=1}^{4}\sin^2 l_\mu \sum_{\nu=1}^{4}\sin^2 l_\nu \sum_{\rho=1}^{4}\cos^2\frac{l_\rho}{2} \right.$$

$$+ \frac{1}{4}c_{sw}^2\sum_{\mu=1}^{4}\sin^2 l_\mu \sum_{\nu=1}^{4}\sin^2 l_\nu \cos^2\frac{l_\nu}{2} - \frac{1}{4}(\tilde{l}^2)^2\sum_{\mu=1}^{4}\cos^2\frac{l_\mu}{2} + \frac{1}{2}\tilde{l}^2\sum_{\mu=1}^{4}\sin^2 l_\mu + \frac{1}{2}c_{sw}\tilde{l}^2\sum_{\mu=1}^{4}\sin^2 l_\mu \sum_{\nu=1}^{4}\cos^2\frac{l_\nu}{2}$$

$$\left. - \frac{1}{2}c_{sw}\tilde{l}^2\sum_{\mu=1}^{4}\sin^2 l_\mu \cos^2\frac{l_\mu}{2} \right], \tag{B13}$$

$$I_N = \int \frac{d^4l}{(2\pi)^4} G(l)S(-l)^2 \left[-\frac{1}{2}\bar{l}^2 \sum_{\mu=1}^{4} \sin^2 l_\mu - \frac{1}{4}(\bar{l}^2)^2 \sum_{\mu=1}^{4} \sin^2 \frac{l_\mu}{2} + \frac{1}{3} \left(\sum_{\mu=1}^{4} \sin^2 l_\mu \sum_{\nu=1}^{4} \cos^2 \frac{l_\nu}{2} \right. \right.$$

$$\left. -4\sum_{\mu=1}^{4} \sin^2 l_\mu \cos^2 \frac{l_\mu}{2} \right) + \frac{1}{3}\left(\frac{1}{2} c_{sw}\bar{l}^2 + \frac{1}{16} c_{sw}^2 (\bar{l}^2)^2 \right)\left(\sum_{\mu=1}^{4} \sin^2 l_\mu \sum_{\nu=1}^{4} \cos^2 \frac{l_\nu}{2} - \sum_{\mu=1}^{4} \sin^2 l_\mu \cos^2 \frac{l_\mu}{2} \right) \right], \tag{B14}$$

where functions $X(l)$, $Y(l)$, and $Z(l)$ in the integrands are

$$X(l) = [e^{il_4}A^{(0)}(l)^n + 1]\frac{1}{2M_0 n} \sum_{m=0}^{n-1} A^{(0)}(l)^m, \tag{B15}$$

$$Y(l) = A^{(0)}(l)^n [e^{il_4} + 1]\frac{ic_4}{4M_0}, \tag{B16}$$

$$Z(l) = A^{(0)}(l)^n [-ie^{il_4/2}]. \tag{B17}$$

There are infra-red divergences in the integrals I_A in Eq. (B1), I_G in Eq. (B7) and I_L in Eq. (B12), for which we subtract a continuum expression from their integrand in the region $l^2 < 1$. We then add back their analytic integral except for the $\ln(a\lambda)$ term, so that I_X becomes finite. When those integrals appear in the expressions of on-shell amplitude, the infra-red divergences will be added.

APPENDIX C: ONE-LOOP FOUR-QUARK AMPLITUDES

The lattice one-loop expression of the perturbative on-shell amplitudes is

$$\langle \bar{b}\Gamma q\bar{b}\Gamma q \rangle = Z_h^{lat}Z_l^{lat}\left[\langle \bar{b}\Gamma q\bar{b}\Gamma q \rangle_0 + \frac{\alpha_s}{4\pi}(X_{heavy-light}^{singlet} + X_{heavy-light}^{octet} + X_{heavy-heavy}^{octet} + X_{light-light}^{octet}), \right] \tag{C1}$$

where Z_l^{lat} and Z_h^{lat} are light and heavy quark wave function renormalizations, respectively, and are given by

$$Z_l^{lat} = 1 + \frac{\alpha_s}{4\pi} C_F[\ln(a^2\lambda^2) + C_l], \tag{C2}$$

$$Z_h^{lat} = 1 + \frac{\alpha_s}{4\pi} C_F[-2\ln(a^2\lambda^2) + C_h]. \tag{C3}$$

The vertex corrections X's are classified by the topology of Feynman diagrams. Figure 2 shows the diagrams in which the gluon line connects heavy and light quarks and the flow of color is closed. The amplitude of these diagrams is denoted as $X_{heavy-light}^{singlet}$. In Fig. 3 the gluon line connects heavy and light quarks, but the color flow is not closed, which we call $X_{heavy-light}^{octet}$. Figures 4 and 5 represent the diagrams in which the gluon line mediates between two heavy quarks or between two light quarks, respectively. The color flow cannot close in these diagrams, and we denote them as $X_{heavy-heavy}^{octet}$ and $X_{light-light}^{octet}$, respectively. The expressions of the one-loop amplitudes are the following:

$$X_{heavy-light}^{singlet} = (4\pi)^2 C_F\left[2\left(I_A - \frac{1}{16\pi^2}\ln(a^2\lambda^2) \right)\langle \bar{b}\Gamma q\bar{b}\Gamma q \rangle_0 + 2I_B\langle \bar{b}\gamma_4\Gamma\gamma_4 q\bar{b}\Gamma q \rangle_0 + 2I_C \sum_{i,j=1}^{3} \langle \bar{b}\gamma_i\gamma_j\Gamma\gamma_j\gamma_i q\bar{b}\Gamma q \rangle_0 \right.$$

$$\left. + 2(I_D + I_F)\sum_{i=1}^{3} \langle \bar{b}\gamma_i\Gamma\gamma_i q\bar{b}\Gamma q \rangle_0 + 2I_E \sum_{i=1}^{3} \langle \bar{b}\gamma_4\gamma_i\Gamma\gamma_i\gamma_4 q\bar{b}\Gamma q \rangle_0 \right], \tag{C4}$$

$$X_{heavy-light}^{octet} = (4\pi)^2\left[2\left(I_A - \frac{1}{16\pi^2}\ln(a^2\lambda^2) \right)\langle \bar{b}\Gamma T^a q\bar{b}\Gamma T^a q \rangle_0 + 2I_B\langle \bar{b}\Gamma\gamma_4 T^a q\bar{b}\gamma_4\Gamma T^a q \rangle_0 \right.$$

$$+ 2I_C \sum_{i,j=1}^{3} \langle \bar{b}\Gamma\gamma_j\gamma_i T^a q\bar{b}\gamma_i\gamma_j\Gamma T^a q \rangle_0 + 2(I_D + I_F)\sum_{i=1}^{3} \langle \bar{b}\Gamma\gamma_i T^a q\bar{b}\gamma_i\Gamma T^a q \rangle_0$$

$$\left. + 2I_E \sum_{i=1}^{3} \langle \bar{b}\Gamma\gamma_i\gamma_4 T^a q\bar{b}\gamma_4\gamma_i\Gamma T^a q \rangle_0 \right], \tag{C5}$$

$$X^{octet}_{heavy-heavy} = (4\pi)^2 \left[\left(I_G - 2\frac{1}{16\pi^2} \ln(a^2\lambda^2) \right) \langle \bar{b}\Gamma T^a q \bar{b}\Gamma T^a q \rangle_0 + I_H \sum_{i=1}^{3} \langle \bar{b}\Gamma \sigma^i T^a q \bar{b}\Gamma \sigma^i T^a q \rangle_0 \right.$$

$$\left. + (I_I + I_J + 2I_K) \sum_{i=1}^{3} \langle \bar{b}\Gamma \gamma^i T^a q \bar{b}\Gamma \gamma^i T^a q \rangle_0 \right], \tag{C6}$$

$$X^{octet}_{light-light} = (4\pi)^2 \left[\left(I_L + \frac{1}{16\pi^2} \ln(a^2\lambda^2) \right) \sum_{\mu,\nu=1}^{4} \langle \bar{b}\Gamma \gamma_\mu \gamma_\nu T^a q \bar{b}\Gamma \gamma_\mu \gamma_\nu T^a q \rangle_0 + I_M \sum_{\mu=1}^{4} \langle \bar{b}\Gamma \gamma_\mu T^a q \bar{b}\Gamma \gamma_\mu T^a q \rangle_0 \right.$$

$$\left. + I_N \langle \bar{b}\Gamma T^a q \bar{b}\Gamma T^a q \rangle_0 \right]. \tag{C7}$$

[1] S. Hashimoto, plenary talk given at 17th International Symposium on Lattice Field Theory (LATTICE 99), Pisa, Italy, 1999, hep-lat/9909136.

[2] UKQCD Collaboration, A. K. Ewing *et al.*, Phys. Rev. D **54**, 3526 (1996).

[3] V. Giménez and G. Martinelli, Phys. Lett. B **398**, 135 (1997).

[4] J. Christensen, T. Draper, and C. McNeile, Phys. Rev. D **56**, 6993 (1997).

[5] V. Giménez and J. Reyes, Nucl. Phys. **B545**, 576 (1999).

[6] J. M. Flynn, O. F. Hernandez, and B. R. Hill, Phys. Rev. D **43**, 3709 (1991).

[7] A. Borrelli and C. Pittori, Nucl. Phys. **B385**, 502 (1992); an error in D_R is corrected in [8,5,9].

[8] UKQCD Collaboration, M. Di Pierro and C. T. Sachrajda, Nucl. Phys. **B534**, 373 (1998).

[9] K-I. Ishikawa, T. Onogi, and N. Yamada, Phys. Rev. D **60**, 034501 (1999).

[10] M. Golden and B. Hill, Phys. Lett. B **345**, 225 (1991).

[11] A. Duncan *et al.*, Phys. Rev. D **51**, 5101 (1995) and references therein.

[12] G. P. Lepage and P. B. Mackenzie, Phys. Rev. D **48**, 2250 (1993).

[13] B. A. Thacker and G. P. Lepage, Phys. Rev. D **43**, 196 (1991); G. P. Lepage, L. Magnea, C. Nakhleh, U. Magnea, and K. Hornbostel, *ibid.* **46**, 4052 (1992).

[14] S. Hashimoto, K-I. Ishikawa, H. Matsufuru, T. Onogi, and N. Yamada, Phys. Rev. D **60**, 094503 (1999).

[15] N. Yamada *et al.*, talk given at 17th International Symposium on Lattice Field Theory (LATTICE 99), Pisa, Italy, 1999, hep-lat/9910006.

[16] C. Bernard, T. Draper, G. Hockney, and A. Soni, Phys. Rev. D **38**, 3540 (1988).

[17] A. Abada *et al.*, Nucl. Phys. **B376**, 172 (1992).

[18] A. Soni, Nucl. Phys. B (Proc. Suppl.) **47**, 43 (1996).

[19] R. Gupta, T. Bhattacharya, and S. Sharpe, Phys. Rev. D **55**, 4036 (1997).

[20] C. Bernard, T. Blum, and A. Soni, Phys. Rev. D **58**, 014501 (1998).

[21] UKQCD Collaboration, L. Lelloouch and C. J. D. Lin, Nucl. Phys. B (Proc. Suppl.) **73**, 357 (1999).

[22] UKQCD Collaboration, L. Lelloouch and C. J. D. Lin, presented at 8th International Symposium on Heavy Flavor Physics (Heavy Flavors 8), Southampton, England, 1999, hep-ph/9912322.

[23] D. Becirevic, D. Meloni, A. Retico, V. Giménez, L. Giusti, V. Lubicz, and G. Martinelli, hep-lat/0002025.

[24] S. Hashimoto, K-I. Ishikawa, T. Onogi, and N. Yamada, Phys. Rev. D **62**, 034504 (2000).

[25] K-I. Ishikawa, T. Onogi, and N. Yamada, talk given at 17th International Symposium on Lattice Field Theory (LATTICE 99), Pisa, Italy, 1999, hep-lat/9909159.

[26] C. J. Morningstar, Phys. Rev. D **48**, 2265 (1993).

[27] B. Sheikholeslami and R. Wohlert, Nucl. Phys. **B259**, 572 (1985).

[28] C. J. Morningstar and J. Shigemitsu, Phys. Rev. D **57**, 6741 (1998); **59**, 094504 (1999).

[29] M. Beneke, G. Buchalla, and I. Dunietz, Phys. Rev. D **54**, 4419 (1996).

[30] M. Beneke, G. Buchalla, C. Greub, A. Lenz, and U. Nierste, Phys. Lett. B **459**, 631 (1999).